

1 **Effect of sporadic destratification, seasonal overturn and**
2 **artificial mixing on CH₄ emissions from a subtropical**
3 **hydroelectric reservoir**

4 **F. Guérin^{1,2,3,*}, C. Deshmukh^{1,4,5,a}, D. Labat¹, S. Pighini^{6,b}, A Vongkhamsao⁶, P.**
5 **Guédant⁶, W. Rode⁶, A. Godon^{6,c}, V. Chanudet⁷, S. Descloux⁷, D. Serça⁴**

6 [1]{Université de Toulouse ; UPS GET, 14 Avenue E. Belin, F-31400 Toulouse, France}

7 [2]{IRD ; UR 234, GET ; 14 Avenue E. Belin, F-31400, Toulouse, France}

8 [3]{Departamento de Geoquímica, Universidade Federal Fluminense, Niteroi-RJ, Brasil}

9 [4]{Laboratoire d'Aérodologie - Université de Toulouse - CNRS UMR 5560; 14 Av. Edouard
10 Belin, F-31400, Toulouse, France}

11 [5]{Centre for Regulatory and Policy Research, TERI University, New Delhi, India}

12 [6]{Nam Theun 2 Power Company Limited (NTPC), Environment & Social Division – Water
13 Quality and Biodiversity Dept.– Gnommalath Office, PO Box 5862, Vientiane, Lao PDR}

14 [7]{Electricité de France, Hydro Engineering Centre, Sustainable Development Dpt, Savoie
15 Technolac, F-73373 Le Bourget du Lac, France}

16 [a]{now at: Nam Theun 2 Power Company Limited (NTPC), Environment & Social Division
17 – Water Quality and Biodiversity Dept.– Gnommalath Office, PO Box 5862, Vientiane, Lao
18 PDR}

19 [b]{now at: Innsbruck University, Institute of Ecology, 15 Sternwartestrasse, A-6020
20 Innsbruck, Austria and Foundation Edmund Mach, FOXLAB-FEM, Via E. Mach 1, IT-38010
21 San Michele all'Adige, Italy}

22 [c]{now at: Arnaud Godon Company, 44 Route de Genas, Nomade Lyon, 69003 Lyon,
23 France}

24
25 *Correspondence to: F Guérin (Frederic.guerin@ird.fr)

26

27

28 **Abstract**

29 Inland waters in general and specifically freshwater reservoirs are recognized as a source of
30 CH₄ to the atmosphere. Although the diffusion at the air-water interface is the most studied
31 pathway, its spatial and temporal variations are poorly documented.

32 We measured temperature and O₂ and CH₄ concentrations every two weeks for 3.5 years at
33 nine stations in a subtropical monomictic reservoir which was flooded in 2008 (Nam Theun 2
34 Reservoir, Lao PDR). Based on these results, we quantified CH₄ storage in the water column
35 and diffusive fluxes from June 2009 to December 2012. We compared diffusive emissions
36 with ebullition from Deshmukh et al. (2014) and aerobic methane oxidation and downstream
37 emissions from Deshmukh et al. (2016).

38 In this monomictic reservoir, the seasonal variations of CH₄ concentration and storage were
39 highly dependent on the thermal stratification. Hypolimnetic CH₄ concentration and CH₄
40 storage reached their maximum in the warm dry season (WD) when the reservoir was
41 stratified. Concentration and storage decreased during the warm wet (WW) season and
42 reached its minimum after the reservoir overturned in the cool dry season (CD). The sharp
43 decreases of CH₄ storage were concomitant with extreme diffusive fluxes (up to 200 mmol m⁻²
44 d⁻¹). These sporadic emissions occurred mostly in the inflow region in the WW season and
45 during overturn in the CD season in the area of the reservoir that has the highest CH₄ storage.
46 Although they corresponded to less than 10% of the observations, these extreme CH₄
47 emissions (>5 mmol m⁻² d⁻¹) contributed up to 50% of total annual emissions by diffusion.

48 During the transition between the WD and WW seasons, a new emission hotspot was
49 identified upstream of the water intake where diffusive fluxes peaked at 600 mmol m⁻² d⁻¹ in
50 2010 down to 200 mmol m⁻² d⁻¹ in 2012. The hotspot was attributed to the mixing induced by
51 the water intakes (artificial mixing). Emissions from this area contributed 15-25% to total
52 annual emissions although they occur on a surface area representative of less than 1% of the
53 total reservoir surface. We highly recommend measurements of diffusive fluxes around water
54 intakes in order to evaluate if such results can be generalized.

55 **1. Introduction**

56 Since the 1990s, hydroelectric reservoirs are known to be a source of methane (CH₄) to the
57 atmosphere. Their contribution to total CH₄ emissions still needs refinement since the

58 discrepancies among estimates is large, ranging from 1 to 12% of total CH₄ emissions (St
59 Louis et al., 2000;Barros et al., 2011). These two estimates are mostly based on diffusive
60 fluxes at the air-water interface and they overlook emissions from the rivers downstream of
61 the dams (Abril et al., 2005;Guerin et al., 2006;Kemenes et al., 2007;Teodoru et al.,
62 2012;Maeck et al., 2013;Deshmukh et al., 2016), CH₄ ebullition (DelSontro et al.,
63 2010;Deshmukh et al., 2014) and emissions from the drawdown area of reservoirs (Chen et
64 al., 2009;Chen et al., 2011) although these pathways could largely dominate diffusion at the
65 surface of the reservoirs.

66 Even if CH₄ diffusion at the surface of reservoir is the best-documented emission pathway,
67 little information is available on spatial and temporal variability of CH₄ emissions by
68 diffusive fluxes. In tropical amictic and well-stratified reservoirs with CH₄-rich hypolimnion,
69 the highest diffusive fluxes are usually observed during dry periods and when the
70 stratification weaken at the beginning of the rainy season (Guerin and Abril, 2007). A study of
71 CH₄ emissions from a dimictic reservoir suggests a potential large outgassing of CH₄ during
72 the overturn (Utsumi et al., 1998b) as it is the case in natural monomictic and dimictic lakes
73 (Kankaala et al., 2007;López Bellido et al., 2009;Schubert et al., 2010;Schubert et al.,
74 2012;Fernández et al., 2014). Such hot moments of emissions (McClain et al., 2003) could
75 contribute 45-80% of annual CH₄ emissions by diffusion (Schubert et al., 2012;Fernández et
76 al., 2014). They are rarely taken into account in carbon budgets since they can only be
77 captured by high frequency monitoring. Spatial heterogeneity of CH₄ emissions at the surface
78 of reservoirs is also very high. It mostly depends on the spatial variations of ebullition that is
79 controlled by sedimentation (DelSontro et al., 2011;Sobek et al., 2012;Maeck et al., 2013).
80 The spatial variability of diffusion in reservoirs is less prominent with a few exceptions of
81 higher emissions (1) in areas where dense forest is flooded (Abril et al., 2005), (2) at shallow
82 sites (<10m) (Zheng et al., 2011;Sturm et al., 2014) and (3) at river inflows (Musenze et al.,
83 2014). However, as it was shown for CO₂ emissions from a tropical hydroelectric reservoir,
84 taking into account both spatial and temporal variability of emissions significantly affect
85 positively or negatively carbon budgets and emission factors (Pacheco et al., 2015).

86 In the framework of a comprehensive project aiming at quantifying greenhouse gas emissions
87 from the Nam Theun 2 Reservoir (NT2R), a recently flooded subtropical reservoir located in
88 Lao People's Democratic Republic (PDR), we studied (1) the spatial and temporal variability
89 of CH₄ ebullitive fluxes (Deshmukh et al., 2014) and (2) the downstream CH₄ emissions
90 (Deshmukh et al., 2016). In the present study, the objective is to quantify the CH₄ diffusive

91 fluxes at the surface of NT2R and evaluate the significance of the diffusive fluxes in total
92 methane emissions in a subtropical monomictic reservoir with a peculiar water intake that
93 artificially mix the water column. The CH₄ emissions were quantified every two weeks during
94 three and a half year (June 2009 to December 2012) based on a monitoring of CH₄
95 concentrations in the reservoir water column. This was performed at nine stations flooding
96 different types of ecosystems. On the basis of these results, we discuss the spatial and
97 temporal variations of the CH₄ emissions by diffusive fluxes and the significance of hotspots
98 and hot moments in the total emissions from the surface of the reservoir.

99 **2. Material and methods**

100 **2.1. Study area**

101 The NT2 hydroelectric reservoir (17° 59' 49" N, 104° 57' 08" E) was built on the Nam Theun
102 River located in the subtropical region of Lao PDR on the Nakai Plateau. A detailed
103 description of this trans-basin hydroelectric reservoir located on the Nakai Plateau is given in
104 Descloux et al. (2014). Basically, the Nam Theun River is dammed (Nakai Dam, ND in
105 Figure 1) and the water from the Nam Theun River is diverted to the Xebang Fai watershed
106 after passing through water intake (WI in Fig 1) to the powerhouse (PH in Fig 1). The WI is
107 located in a 130 m-width and 9 to 20 m-deep channel on the southwest side on the reservoir
108 and it is located 5 m above the bottom (Figure S1). The powerhouse is located in the valley
109 200 m below the plateau. The filling of the reservoir began in April 2008 with full water level
110 reached by October 2009 and the power plant commissioned in April 2010.. After that date,
111 turbines were turned on and water was continuously delivered to the turbines and downstream
112 of the reservoir. Annually, the NT2 Reservoir receives around 7527 Mm³ of water from the
113 Nam Theun watershed, which is more than twice the volume of the reservoir (3908 Mm³). A
114 continuous flow of 2 m³ s⁻¹ (and occasionally spillway release) is discharged from the Nakai
115 Dam (ND in Fig 1) to the Nam Theun River. This low water discharge corresponds to the
116 minimum water discharge of the Nam Theun River before the dam was built.

117 Typical meteorological years are characterized by three seasons: warm wet (WW) (mid June-
118 mid October), cool dry (CD) (mid October-mid February) and warm dry (WD) (mid
119 February-mid June). Daily air temperature varies between 14°C (CD season) to 30°C (WD
120 season). The mean annual rainfall is about 2400 mm and occurs mainly (80%) in the WW
121 season.

122 During the filling of the reservoir, 489 km² of soils and different types of vegetation
123 (Descoux et al., 2011) were flooded by the end of October 2008. The water level in the
124 reservoir was nearly constant from October 2009 to April 2010 (Figure 2a). After the
125 commissioning (from April 2010 to December 2012) the reservoir surface varied seasonally
126 by a factor of three and reached its maxima (489 km²) and minima (168 to 176 km² depending
127 on the years) during the WW and WD seasons, respectively (Figure 2a). The average water
128 volume is 2.65 km³ with the lowest volume by the end of the WD season (0.71 in June 2011)
129 and the highest at the end of the rainy seasons (3.97 km³ in September 2011) (Figure 2b). The
130 seasonal water level variations are about 10 m (Figure 2c), the average depth is 8 m for a
131 maximum depth of 39 m close to the Nakai Dam.

132 **2.2. Sampling strategy**

133 A total of nine stations (RES1-9, Figure 1) located in the reservoir were monitored every two
134 weeks (fortnightly) in order to determine the vertical profiles of temperature and O₂ and CH₄
135 concentration in the water column. The type of ecosystems flooded, the depth range and the
136 hydrology of the stations are given in the Table 1. Basically, three stations are located on the
137 thalweg of the former Nam Theun River (RES2, RES4, RES6) whereas four other stations are
138 located in a small embayment in the flooded dense forest (RES3), flooded degraded forest
139 (RES5), flooded swamp area (RES7) and flooded agricultural land (RES8). The RES1 station
140 is located 100 m upstream of the Nakai Dam, and RES9 station is located 800 m upstream of
141 the water intake (WI) delivering the water to the powerhouse (Figure 1 and Figure S1). The
142 station RES9 is under the influence of the water column mixing induced by the water
143 withdrawal at the WI, located at the bottom of the reservoir (5m above the bottom) and under
144 10 to 20 m of water (see discussion). All samples and in situ measurements were taken in the
145 morning or early afternoon from an anchored boat. Most of the time, the boat was attached to
146 a buoy at the sampling station. When no buoy was present, an anchor was used with care in
147 order not to re-suspend surface sediments. As the sampling started from the surface, the
148 bottom water was sampled almost an hour later and should not be influenced by the
149 perturbation generated by the anchor.

150 **2.3. Experimental methods**

151 **2.3.1. Vertical profiles of oxygen and temperature**

152 Vertical profiles of O₂ and temperature were measured in situ at all sampling stations with a
153 multi-parameter probe Quanta[®] (Hydrolab, Austin, Texas) since June 2009. In the reservoir,
154 the vertical resolution was 0.5 m above the oxic–anoxic limit and 1 to 5 m in the hypolimnion.

155 **2.3.2. Methane concentration in water**

156 The evolution of CH₄ concentrations has been monitored every two weeks from May 2009 to
157 December 2012. Surface samples were taken with a surface custom-built water sampler (Abril
158 et al., 2007). Other samples from the water column were taken with an Uwitec water sampler
159 at 3m-depth, at the oxic-anoxic interface 1m above and below the oxic-anoxic interface and
160 every 3 to 5m down to 0.5 m above the bottom. Water samples were stored without air bubble
161 in serum glass vials, capped with butyl stoppers, sealed with aluminium crimps and preserved
162 with HgCl₂ (Guerin and Abril, 2007). Samples were analysed within 15 days. Before gas
163 chromatography analysis for CH₄ concentration, a N₂ headspace was created and the vials
164 were vigorously shaken to ensure an equilibration between the liquid and gas phases. The
165 concentration in the water was calculated using the solubility coefficient of Yamamoto et al.
166 (1976).

167 **2.3.3. Gas chromatography**

168 Analysis of CH₄ concentrations were performed by gas chromatography (SRI 8610C gas
169 chromatograph, Torrance, CA, USA) equipped with a flame ionization detector. A subsample
170 of 0.5 ml from the headspace of water sample vials was injected. Commercial gas standards
171 (10, 100 and 1010 ppmv, Air Liquid "crystal" standards) were injected after analysis of every
172 10 samples for calibration. Duplicate injection of samples showed reproducibility better than
173 5%.

174 **2.4. Water column CH₄ storage**

175 Between sampling depths of the vertical CH₄ profiles, concentrations were assumed to change
176 linearly in order to calculate the concentration in each 1-m layer of water. The volume of
177 water in each layer was calculated using the volume-capacity curve (NTPC, 2005). The CH₄

178 storage was calculated by multiplying the average CH₄ concentrations of each layer by the
179 volume of the layer and summing-up the amount of CH₄ for all depth intervals.

180 **2.5. Aerobic CH₄ oxidation**

181 The depth-integrated CH₄ oxidation rates at each station were calculated on the basis of the
182 specific oxidation rates (d⁻¹) determined at NT2R (Deshmukh et al., 2016) and vertical CH₄
183 and O₂ profiles in the water column as already described in (Guerin and Abril, 2007). The
184 depth-integrated CH₄ oxidation rates at each station were estimated only from January 2010
185 since the vertical resolution of the vertical profiles of O₂ and CH₄ was not high enough in
186 2009.

187 As the aerobic methane oxidation rates we obtained were potential, CH_{4-ox} were corrected for
188 two limiting factors, the oxygen availability and the light inhibition as described in Guerin
189 and Abril (2007). The final equation to compute in situ oxidation rates (CH_{4-ox}, mmol m⁻² d⁻¹)
190 is:

$$191 \text{CH}_{4\text{-ox}} = C_{\text{CH}_4} \cdot S_{\text{CH}_4\text{-ox}} \cdot C_{\text{O}_2} / (C_{\text{O}_2} + K_{\text{m}(\text{O}_2)}) \cdot d \cdot I(z)$$

192 with C_{CH₄}, the CH₄ concentration; S_{CH_{4-ox}}, the specific CH_{4-ox} from Deshmukh et al. (2016);
193 C_{O₂}, the oxygen concentration; K_{m(O₂)}, the half-saturation constant (K_m) of O₂ for CH₄
194 oxidation, d, depth of the water layer and I(z), the inhibition of methanotrophic activity by
195 light as defined by Dumestre et al. (1999) at the Petit Saut Reservoir. Finally, the CH₄
196 oxidation rates were integrated in the oxic water column, from the water surface to the limit of
197 oxygen penetration.

198 **2.6. Diffusive fluxes from surface concentrations**

199 The diffusive CH₄ fluxes were calculated from the monitoring of surface concentrations with
200 the thin boundary layer (TBL) equation at all stations in the reservoir (RES1-9). The CH₄
201 surface concentrations in water and the average CH₄ concentration in air (1.9 ppmv) obtained
202 during eddy covariance deployments (Deshmukh et al., 2014) were applied in equation (1) to
203 calculate diffusive flux:

$$204 \quad F = k_T \times \Delta C \quad (1)$$

205 where F , the diffusive flux at water-air interface; $\Delta C = C_w - C_a$, the concentration gradient
206 between the water (C_w) and the concentration at equilibrium with the overlying atmosphere
207 (C_a) and k_T , the gas transfer velocity at a given temperature (T):

$$208 \quad k_T = k_{600} \times (600/Sc_T)^n \quad (2)$$

209 with Sc_T , the Schmidt number of CH_4 at a given temperature (T) (Wanninkhof, 1992); n , a
210 number that is either $2/3$ for low wind speed ($< 3.7 \text{ m s}^{-1}$) or $1/2$ for higher wind speed and
211 turbulent water (Jahne et al., 1987).

212 For the determination of k_{600} at the stations RES1-8, we averaged the formulations from
213 Guerin et al. (2007) which includes the cumulative effect of wind (U_{10}) and rain (R) on k_{600}
214 ($k_{600} = 1.66e^{0.26U_{10}} + 0.66R$), and the formulation of MacIntyre et al. (2010) ($k_{600} = 2.25 U_{10}$
215 $+ 0.16$) whatever the buoyancy fluxes. As shown by Deshmukh et al. (2014), the average of
216 the fluxes obtained from these two relationships compared well with fluxes measured by
217 floating chambers at the reservoir surface during three deployments at NT2R. Since the water
218 current velocities were lower than 1 cm s^{-1} in most of the reservoir (Chanudet et al., 2012), the
219 effect of water current on k_{600} was not included. The average wind speed (at 10 m height) and
220 rainfall from two meteorological stations located at the Ban Thalang Bridge (close to RES4
221 station,) and close to the WI (Figure 1) was used for the calculation of fluxes all stations
222 (RES1-8). On average for all stations and all sampling date, the k_{600} was $5.6 \pm 5.3 \text{ cm h}^{-1}$
223 ranging between 0.91 to 40.4 cm h^{-1} . The lowest k_{600} were calculated in the CD season
224 ($3.43 \pm 1.01 \text{ cm h}^{-1}$; 1.65 - 6.06 cm h^{-1}) while the highest were obtained during the WW season
225 ($6.78 \pm 6.33 \text{ cm h}^{-1}$; 1.57 - 40.42 cm h^{-1}) due to high rainfall (up to 113 mm day^{-1}). In the WD
226 season k_{600} averaged $5.58 \pm 4.81 \text{ cm h}^{-1}$. This average k_{600} is significantly enhanced by some
227 rainy events in late May-early June in 2010 and 2012 (up to 60 mm d^{-1}).

228 At the water intake (RES9) where the hydrology and hydrodynamics is different from the
229 other stations, it was impossible to quantify the k_{600} since the boat drifted quickly to the
230 shoreline because of water currents in the narrow channel (Figure S1). According to Chanudet
231 et al. (2012), water current velocity in this area of the reservoir is about 0.2 m s^{-1} . After
232 Borges et al. (2004), the contribution of such water currents in a water body with depth
233 ranging from 9 to 20 m is $2.0 \pm 0.5 \text{ cm h}^{-1}$ which should be summed up with the contribution of
234 wind and rainfall from Guerin et al. (2007) and MacIntyre et al. (2010). It gives an average of
235 9 cm h^{-1} . The k_{600} was determined in the regulating dam located downstream of the turbine
236 where we visually observed vortexes similar to those observed at RES9. In the regulating

237 dam, the k_{600} obtained in May 2009 and March 2010 with a drifting floating chamber as
238 described in Deshmukh et al. (2014) was 19 cm h^{-1} on average for 4 measurements ranging
239 from 9 to 40 cm h^{-1} . In order to be conservative for the estimation of emissions from the water
240 intake, we considered a constant value of k_{600} (10 cm h^{-1}) which is in the lower range of (1)
241 the k_{600} calculated from (Guerin et al., 2007), MacIntyre et al. (2010) and Borges et al. (2004),
242 and (2) k_{600} values determined in the regulating dam that we consider as an area with
243 comparable hydrology/hydrodynamics.

244 **2.7. Total emissions by diffusive fluxes**

245 Based on physical modelling (Chanudet et al., 2012), it has been shown that the station RES9
246 located at the water intake is representative of an area of $\sim 3 \text{ km}^2$ (i.e. 0.6% of reservoir water
247 surface), whatever the season. This 3- km^2 area was used to extrapolate specific diffusive
248 fluxes from RES9. The embayment where RES3 is located represents a surface area of 5-6%
249 of the total surface area of the reservoir whatever the season (maximum 28 km^2), to which
250 were attributed the specific diffusive fluxes from RES3. The diffusive fluxes calculated for
251 RES1, RES2, RES4, RES5, RES6, RES7 and RES8 stations were attributed to the water
252 surface area representative for each station, taking into account the seasonal variation of the
253 reservoir water surface from the surface-capacity curve (NTPC, 2005).

254 **2.8. Statistical and correlation analysis**

255 Statistical tests were performed to assess the spatial and temporal variations in the surface
256 CH_4 concentrations and diffusive fluxes at all stations in the reservoir. Normality of the
257 concentration and diffusive datasets was tested with R software (R Development Core Team,
258 2008) and the Nortest package (Gross and Ligges, 2015). The data distribution was tested
259 with the Fitdistrplus package (Delignette-Muller et al., 2015).

260 Since all tests indicated that the distribution of the data were neither normal nor lognormal,
261 Kruskal-Wallis and Mann-Whitney tests were performed with GraphPad Prism (GraphPad
262 Software, Inc., v5.04). No significant differences were found between the seasons and/or the
263 stations. These test results were attributed to the very large range of surface concentrations
264 due to the sporadic occurrence of extreme values (over 4 orders of magnitude). In order to
265 reduce this range, the log of the concentrations was used. For each station, the time series of
266 the log of the CH_4 surface concentrations were linearly interpolated and re-sampled every 15
267 days in order to compare time series with the same number of observations. The log of the

268 concentrations was used to determine the frequency distribution, the skewness of the dataset
269 (third order moment), the auto-correlation of each time series and the correlation between the
270 different stations. All analyses were performed using Matlab.

271 3. Results

272 3.1. Temperature and O₂ dynamics in the reservoir

273 During the three and half year of monitoring at the stations RES1-8, the NT2R was thermally
274 stratified with a thermocline at 4.5 ± 2.6 m depth in the WD (Feb-Jun) season as revealed by
275 the vertical profiles of temperature (Figure 3). In the WW season, the temperature vertical
276 profiles at the stations RES1-8 either showed a thermocline (RES7 and RES8 in 2010 and
277 2011, Figure 3) whereas in some occasions, the temperature decreased regularly from the
278 surface to the bottom during sporadic destratification (RES1-3, Figure 3). On average during
279 the WW season, a thermocline was located at 5.8 ± 4.8 m depth. During the CD season, the
280 reservoir overturned as already mentioned by Chanudet et al. (2012) and the temperature was
281 constant from the surface to the bottom (Figure 3) in the different years. In order to illustrate
282 the destratification, a stratification index (ΔT) which corresponds to the difference between
283 the surface and bottom water temperature was defined (Figure 4a). During the periods of
284 stratification in the WD seasons, ΔT was up to 10°C higher than during reservoir overturn in
285 the CD season with ΔT close to zero (Figure 4a). During the WW season, the ΔT decreased
286 gradually which means that the overturn occurred over several months.

287 During the WD season at the stations RES1-8, an oxycline was most of the time located at a
288 depth concomitant with the depth of the thermocline whereas oxygen penetrated deeper in the
289 WW season (Figure 3). During these two seasons, the epilimnion was always well oxygenated
290 with O₂ concentrations higher than 200 $\mu\text{mol L}^{-1}$. In the WD season, the hypolimnion was
291 completely anoxic whereas O₂ reached occasionally the hypolimnion during the sporadic
292 destratification events in the WW season ($29 \pm 54 \mu\text{mol L}^{-1}$, Figure 3 and 4b). During the CD
293 season (reservoir overturn), the water column was often oxygenated from the top to the
294 bottom of the reservoir (Figure 3). On average over the whole reservoir, the lowest
295 hypolimnic oxygen concentration was observed in 2010 before the reservoir was
296 commissioned (Figure 4b).

297 After the commissioning of the reservoir and the turbines were powered on in April 2010, the
298 water column located near the intake (RES9) completely mixed as indicated by the

299 homogeneous temperature and oxygen profiles with depth in every season (Figure 3). The
300 water column at RES9 was always well oxygenated ($163 \pm 62 \mu\text{mol L}^{-1}$, Figure 3).

301 **3.2. Seasonal dynamics of the CH₄ concentration in the reservoir**

302 At the station RES1-8, when the water column is thermally stratified with a steep oxicleine in
303 the WD and often in the WW seasons, CH₄ concentrations are on average ~150 times higher
304 in the reservoir hypolimnion ($246 \pm 234 \mu\text{mol L}^{-1}$) than in the epilimnion ($1.6 \pm 7.7 \mu\text{mol L}^{-1}$)
305 (Figure 3). The gradient of CH₄ concentration at the thermocline/oxicleine was steeper during
306 the WD season than during the WW season (Figure 3). During the CD season, the average
307 CH₄ concentration in the reservoir bottom water lowered by a factor of three compare to the
308 WD and the WW seasons. However, the reservoir overturn increased the average CH₄
309 concentrations in the epilimnion by a factor of two ($3.4 \pm 14.8 \mu\text{mol L}^{-1}$) in comparison with
310 the WD and WW seasons. After the commissioning, the CH₄ vertical profiles of concentration
311 before turbine intake (RES9) were homogeneous from the surface to the bottom. The highest
312 average CH₄ concentration from the surface to the bottom peaked up to $215 \mu\text{mol L}^{-1}$ in July
313 2010 at this station. On a seasonal basis, the CH₄ concentration at RES9 averaged 39.8 ± 48.8 ,
314 29.9 ± 55.4 and $1.9 \pm 4.3 \mu\text{mol L}^{-1}$ during the WD, WW and CD seasons, respectively (Figure
315 3). The concentrations at RES9 were up to 10 times lower than the maximum bottom
316 concentrations at the other stations for a given season. Since the station RES9 behaved
317 differently from the other stations, results from this station will be treated separately.

318 The overall bottom CH₄ concentration (Figure 4c) and dissolved CH₄ stock in the reservoir
319 (Figure 4d) increased at the beginning of the WD season. The higher bottom CH₄
320 concentration and storage in the reservoir are concomitant with the establishment of anoxia in
321 the hypolimnion and thermal stratification (Figure 4). Hypolimnic CH₄ concentration and
322 storage reached their maxima (up to $508 \pm 254 \mu\text{mol L}^{-1}$ and $4.7 \pm 0.5 \text{Gg}(\text{CH}_4)$, Figure 4c,d)
323 at the end of the WD-beginning of the WW season when the residence time of water in the
324 reservoir was the lowest (40 days, Figure 4d) and when the reservoir volume was the smallest
325 (Figure 2b). Along the WW season, the thermal stratification weakened (Figure 4a) and the
326 CH₄ concentration and dissolved CH₄ stock decreased (Figure 4c,d) while the residence time
327 of water increased (Figure 4d) and the water volume increased (Figure 2b). In the CD season,
328 the reservoir overturns as evidenced by the low ΔT and the penetration of O₂ to the
329 hypolimnion (Figure 4a,b). During CD season, the bottom CH₄ concentration and the storage
330 reached their minima (down to $1.3 \pm 4.5 \mu\text{mol L}^{-1}$ and $0.01 \pm 0.001 \text{Gg}(\text{CH}_4)$, Figure 4c,d)

331 when the residence time of water was the longest (Figure 4d). The sharp decrease of CH₄
332 storage and concentration in the transition from the WW to the CD seasons is concomitant
333 with a sharp increase of O₂ concentration at the bottom (up to $160 \pm 89 \mu\text{mol L}^{-1}$, Figure 4).

334 During the three and a half years of monitoring, the same seasonal pattern as described above
335 is observed although the annual CH₄ bottom concentration and storage was threefold higher in
336 2009 and 2010 than in the year 2011 (Figure 4c,d). In the dry year 2012, the reservoir bottom
337 CH₄ concentration and storage was almost twice higher than in wet year 2011.

338 **3.3. Aerobic CH₄ oxidation in the reservoir**

339 Between 2010 and 2012, the depth integrated aerobic CH₄ oxidation rates ranged between
340 0.05 and 380 mmol m⁻² d⁻¹ at the stations RES1-RES8 (Figure 5). On average, aerobic
341 oxidation was higher in the WW season ($55 \pm 63 \text{ mmol m}^{-2} \text{ d}^{-1}$) than in the CD ($30 \pm 46 \text{ mmol}$
342 $\text{m}^{-2} \text{ d}^{-1}$) and WD ($36 \pm 32 \text{ mmol m}^{-2} \text{ d}^{-1}$) seasons and it was not statistically different for the
343 three years. In the WD season, aerobic CH₄ oxidation was on average twice higher in 2010
344 than for the two following years. In the CD season of the year 2012, the aerobic oxidation rate
345 were exceptionally high compare to the same season in the previous years.

346 **3.4. Spatial and seasonal variability of surface CH₄ concentration and diffusive fluxes** 347 **at the reservoir surface (RES1-RES8)**

348 The surface concentrations at the stations RES1-8 ranged from 0.02 to 150 $\mu\text{mol L}^{-1}$ and were
349 $2.0 \pm 10.5 \mu\text{mol L}^{-1}$ (median = 0.9), $1.5 \pm 5.5 \mu\text{mol L}^{-1}$ (median = 0.4) and $3.4 \pm 14.7 \mu\text{mol L}^{-1}$
350 (median = 0.2) on average for the CD, WD and WW season, respectively. The surface
351 concentration followed a loglogistic distribution, which indicates the existence of extremely
352 high values. This is confirmed by the fact that the skewness of the time series of the log of the
353 CH₄ concentrations for all stations is positive (Figure S2), especially at the stations RES1,
354 RES3 and RES7 for which the skewness is >1 (Figure S2). Over the course of the three and a
355 half year of survey, the surface concentrations were not statistically different between all
356 stations and no statistically significant seasonal variations were observed because of the
357 occurrence of sporadic events in all season (Figure S3a). The normalized distribution of
358 concentrations (in log) according to seasons (Figure 6) indicates that these high
359 concentrations were observed without any clear seasonal trend at the station RES1, RES5 and
360 RES6 (<1 up to 150 $\mu\text{mol L}^{-1}$). At the stations RES2 and RES3, the concentrations up to 128

361 $\mu\text{mol L}^{-1}$ were mostly observed in the CD season when the reservoir overturns. At the station
362 RES4 located at the Nam Xot and Nam Theun confluence and at the stations RES7 and RES8
363 both located in the inflow region of the Nam Theun River, the high surface concentrations (up
364 to $64.60 \mu\text{mol L}^{-1}$) were mostly observed during the WW season when the reservoir
365 undergoes sporadic destratification. The auto-correlation function of the time series of the log
366 of the surface CH_4 concentrations and diffusive fluxes at the stations RES1-8 indicated that all
367 stations (except RES1) have a memory effect of 30 to 40 days (Figure S4). This implies that
368 with a sampling frequency of 15 days, we captured most of the changes in the surface CH_4
369 concentrations. At station RES1, the changes in CH_4 concentrations are faster than at other
370 stations and would have deserved a monitoring with a frequency higher than 15 days.

371 During the monitoring at RES1-RES8 stations, the average diffusive flux was 2.8 ± 12.2
372 $\text{mmol m}^{-2} \text{d}^{-1}$ ranging from 0.01 to $201.86 \text{mmol m}^{-2} \text{d}^{-1}$ without any clear interannual and
373 seasonal trends (Figure S3b). As for the concentrations, flux data followed a loglogistic
374 distribution. The median flux in the WD season is 40 to 80% higher than the median in the
375 WW and CD season, respectively. During the WW and the CD seasons, more than 60% of the
376 calculated fluxes were lower than $1 \text{mmol m}^{-2} \text{d}^{-1}$, which corresponds to classical flux in
377 pristine rivers. However, the average fluxes in the WW and CD season are 30% higher than in
378 the WD season (Table 2). This confirms the presence of extremely high values during WD
379 and CD seasons, as expected from the surface concentrations. All seasons together, around
380 7% of the diffusive fluxes that we observed were higher than $5 \text{mmol m}^{-2} \text{d}^{-1}$ which
381 corresponds to extremely high diffusive fluxes in comparison with data from the literature for
382 reservoirs and lakes (Bastviken et al., 2008;Barros et al., 2011). The median and average of
383 these extreme fluxes higher than $5 \text{mmol m}^{-2} \text{d}^{-1}$ were 2 times higher in the WW and CD
384 seasons than in the WD season (Table 2).

385 At NT2R, diffusive CH_4 fluxes covered the whole range of fluxes reported for tropical
386 reservoirs, depending on the season. Most of the fluxes at the NT2R Reservoir were around
387 one order of magnitude lower than those at Petit Saut Reservoir (French Guiana) just after the
388 impoundment (Galy-Lacaux et al., 1997), and in the same order of magnitude as reported for
389 reservoirs 10 to 18 years older (Abril et al., 2005;Guerin et al., 2006;Kemenes et al.,
390 2007;Chanudet et al., 2011). However, some diffusive fluxes at the stations RES1-8 in the
391 WW and the CD seasons (up to $202 \text{mmol m}^{-2} \text{d}^{-1}$) are among the highest ever reported at the

392 surface of a hydroelectric reservoir or a lake (Bastviken et al., 2011;Barros et al., 2011) and
393 rivers downstream of dams (Abril et al., 2005;Guerin et al., 2006;Deshmukh et al., 2016).

394 **3.5. Surface methane concentrations and diffusive fluxes at the water intake (RES9)**

395 After the commissioning of the reservoir (Julian day 450), the concentrations at the stations
396 RES9 (Figure 7a) located at the water intake were up to 30 times higher than at any other
397 stations Following the commissioning of the reservoir and powering of the turbines, CH₄
398 concentrations at station RES9, which was located at the water intake, were up to 30 times
399 higher than at the other stations (Figure 7a). On average CH₄ concentrations were 36.6±35.8
400 μmol L⁻¹ (median = 24.3), 37.6±67.0 μmol L⁻¹ (median = 0.9) and 1.0±1.7 μmol L⁻¹ (median
401 = 0.3) in the WD, WW and CD season, respectively. The surface concentrations at RES9 were
402 significantly higher in the WD and WW seasons than in the CD season (p = 0.0002 and
403 Figure 7a). The highest concentration was observed each year at the end of the WD season-
404 beginning of the WW season in between June and August. These maxima decreased from 215
405 μmol L⁻¹ in August 2010 to 87 μmol L⁻¹ in June 2012.

406 The diffusive fluxes ranged between 0.03 and 605.38 mmol m⁻² d⁻¹ (Figure 7b and Table 2).
407 On average, the CH₄ diffusive fluxes at RES9 were two to forty times higher than at the other
408 stations in the CD, WD and WW season. Diffusive fluxes at this station are usually higher
409 than 10 mmol m⁻² d⁻¹ from April to July that corresponds to the WD season and the very
410 beginning of the WW season. In 2010, diffusive fluxes were on average 241 ± 219 and 239 ±
411 228 mmol m⁻² d⁻¹ respectively for the WD and WW seasons. In 2011 and 2012, the fluxes
412 dropped down by a factor of two in the WD season (112 ± 110 mmol m⁻² d⁻¹) and almost by a
413 factor of forty in the WW season (6.8 ± 14.4 mmol m⁻² d⁻¹). Overall, emissions at RES9
414 decreased by a factor of two between 2010 and 2012.

415 **4. Discussion**

416 **4.1. CH₄ dynamic in the reservoir water column**

417 The gradual decrease of the CH₄ concentration from the anoxic bottom water column to the
418 metalimnion and the sharp decrease around the oxicleine in the metalimnion (Figure 3) is
419 typical in reservoirs and lakes where CH₄ is produced in anoxic sediments and flooded soils
420 (Guerin et al., 2008;Sobek et al., 2012;Maeck et al., 2013), and where most of it is oxidized at

421 the oxic-anoxic interface (Bedard and Knowles, 1997; Bastviken et al., 2002; Guerin and Abril,
422 2007; Deshmukh et al., 2016).

423 CH₄ concentrations and storage increase concomitantly with the surface water temperature
424 and the establishment of the thermal stratification during the WD season and peak at the end
425 of the WD season-beginning of the WW season when the surface and the volume of the
426 reservoir was minimum (Figure 2, 3 and 4). The fact that the storage reached its maximum
427 when the reservoir volume is at its minimum shows that the increase of concentration at the
428 bottom of the reservoir is highly significant. During the WW season, CH₄ concentrations and
429 storage decrease slowly (Figure 4) while aerobic methane oxidation reaches its maximum
430 (Figure 5). When the reservoir overturns at the beginning of the CD season, the CH₄
431 hypolimnetic concentrations and storage reach their minima (Figure 4). The overturn favours
432 the penetration of oxygen down to the bottom (Figure 3 and 4b). The sharp decrease of the
433 CH₄ concentrations and CH₄ storage during this period is expected to result from sudden
434 outgassing (Section 4.2) together with an enhancement of the aerobic CH₄ oxidation as
435 observed in lakes that overturn (Utsumi et al., 1998b; Utsumi et al., 1998a; Kankaala et al.,
436 2007; López Bellido et al., 2009; Schubert et al., 2010; Schubert et al., 2012; Fernández et al.,
437 2014). Significant increase in methane oxidation during overturn in the CD season was not
438 observed except for the year 2012 (Figure 5) when hypolimnetic CH₄ concentrations were still
439 quite high (Figure 4c,d). The absence of a clear enhancement of the CH₄ oxidation in the
440 water column of NT2R can be attributed to the slow erosion of the thermal stratification
441 before the reservoir really overturns.

442 As the reservoir overturns during the period over which the water residence time is the
443 longest, the temporal evolution of the concentrations is anti-correlated with the residence time
444 (Figure 4c,d). The seasonal dynamics of the CH₄ in the monomictic NT2R differs from
445 permanently stratified reservoirs like Petit Saut Reservoir where CH₄ concentration increased
446 with retention time (Abril et al., 2005). However, at the annual scale the water residence time
447 has a strong influence on CH₄ concentration and storage in the reservoir. Before the reservoir
448 was commissioned (April 2010), the water residence time was up to 4 years and the CH₄
449 storage was up to four times higher than in 2011 and 2012 (Figure 4d). Although a decrease
450 of concentration and storage with the age of the reservoir was expected (Abril et al., 2005),
451 storage in the dry year of 2012 was twice that of the wet year of 2011, likely due to a 25%
452 increase in residence time between 2011 and 2012 due to a decrease in rainfall and water
453 inputs. In wet years like 2011, the thermal stratification is weaker than in dry years since the

454 warming of the epilimnion is less efficient due to (1) lower insulation and cold water inputs
455 from above and (2) the high riverine inputs of water alters the stability of the reservoir
456 thermal stratification as shown by the sharper decrease of the thermal stratification illustrated
457 by the decrease of the stratification index (ΔT) in 2011 than in 2012 (Figure 4a). As a
458 consequence, the oxygen diffusion to the hypolimnion was higher in 2011 than in 2012
459 (Figure 4b) and it enhanced aerobic methane oxidation by 20% in the water column in the
460 WW season in 2011 as compared to 2012 (Figure 5). Therefore our results suggest that the
461 hydrology affects both the thermal stratification and therefore the diffusion of O_2 in the water
462 column. The enhancement of O_2 penetration in rainy years favours the CH_4 oxidation and
463 therefore contributes to the CH_4 storage reduction. With less CH_4 in the water column, the
464 potentiality for downstream emissions (Deshmukh et al., 2016) and emissions through
465 hotspots and hot moments (see below) is highly reduced.

466 **4.2. Hot moments of emissions during sporadic destratification and reservoir overturn**

467 Figure 8 illustrates the evolution of the diffusive fluxes, the stratification index (ΔT), the CH_4
468 storage and the aerobic CH_4 oxidation at the stations RES1, RES3, RES7 and RES8. These
469 four stations were selected for their contrasting skewness (Figure S2) which gives an
470 indication on the occurrence of extreme events and the facts that they are representative for all
471 station characteristics (Table 1). It shows that the large bursts of CH_4 (from 5 up to 200 mmol
472 $m^{-2} d^{-1}$) always occurred in both the CD and WW seasons only when ΔT decreased sharply
473 ($>4^\circ C$, Figure 8a,d,g,j) and were usually followed by a sharp decrease of the CH_4 storage in
474 the water column (Figure 8b,e,h,k).

475 Hot moments of emissions occurred during overturn in the CD at the stations RES1 and RES3
476 as illustrated in Figure 7. We therefore confirm the occurrence of hot moments of emissions
477 during the reservoir overturn in the CD season as already observed in lakes that overturn in
478 temperate regions (Kankaala et al., 2007;López Bellido et al., 2009;Schubert et al.,
479 2010;Schubert et al., 2012;Fernández et al., 2014). The highest emissions determined at
480 NT2R are one order of magnitude higher than previously reported outgassing during overturn
481 and they occur mostly in the section of the reservoir that has the longest water residence time
482 (RES1-3, Table 1) and the largest CH_4 storage (Figure 8b,e,h,k). This suggests that the impact
483 of reservoir overturn can be very critical for the whole-reservoir CH_4 budget in tropical
484 hydroelectric reservoirs and especially in young ones where hypolimnic concentration could
485 reach up to 1000 $\mu mol L^{-1}$.

486 Hot moments of emissions also occur during sporadic destratifications in the WW season in
487 the inflow region (RES4 and RES6-8) where the inflow of cool water from the watershed
488 might disrupt the thermal stratification in reservoirs (see stations RES7 and 8 in Figure 8).
489 This is contrasting with the observations in reservoir older than NT2R where high emissions
490 from the inflow region were recently attributed to an enhancement of CH₄ production fuelled
491 by the sedimentation of organic matter from the watershed (Musenze et al., 2014).

492 In the WD season, some sporadic emissions occurred but they were always lower than 20
493 mmol m⁻² d⁻¹ that is up to ten times lower than extreme fluxes in the WW and CD season.
494 Those high fluxes occurred at RES3, RES7 and RES8 (Figure 8d,g,j) and were associated
495 with ΔT variations lower than 2°C. The CH₄ storage decreases associated with these fluxes,
496 however, were not as sharp as those observed during other seasons (Figure 8e,h,k). These
497 high emissions were actually associated with early rains and associated high winds that occur
498 sometimes in the last fifteen days of May. This shows that a moderate erosion of the
499 stratification when hypolimnetic CH₄ concentrations are high could enhance vertical transport
500 of CH₄ toward the surface and emissions to the atmosphere.

501 Basically, this intense monitoring shows that spatial and temporal variations of CH₄ emissions
502 are largely controlled by the hydrodynamics of the reservoir with extreme emissions
503 occurring (1) in the inflow region during the wet season and (2) in area away from inflow
504 zone during reservoir overturns in the CD season. Even if less frequent, moderate erosion of
505 the stable and steep thermal stratification during warm seasons, could also lead to high
506 emissions.

507 The evolution of depth-integrated aerobic CH₄ oxidation is not clearly related with the
508 reservoir overturns and the CH₄ burst (Figure 8). Significant increases in the aerobic CH₄
509 oxidation occurred mostly during the first half of the WD season when the stratification was
510 unstable and at the very beginning of the destratification in the WW, when ΔT started to
511 decrease. The oxidation could reach high values (up to 380 mmol m⁻² d⁻¹) during these two
512 periods since the yield of CH₄ in the water column to sustain the activity of methanotrophs is
513 higher than in the CD season when the reservoir overturns. It shows that in reservoirs or lakes
514 like NT2R that destratify progressively before the overturn, there is no substantial increase of
515 the CH₄ oxidation when the water body finally overturns as was observed in lakes that
516 overturn within a few days (Kankaala et al., 2007). In addition, the contribution of CH₄
517 oxidation to the total loss of CH₄ (sum of diffusion and oxidation) in the WD and WW

518 seasons was 90-95% during the entire monitoring whereas it was 85% in the CD season.
519 Therefore, during overturn in the CD season, a significant amount of CH₄ is oxidized, but the
520 removal of CH₄ during overturn is not as efficient as during seasons with a well-established
521 thermal stratification.

522 During the periods with major loss in the CH₄ storage with concomitant CH₄ burst, we
523 compared the change in the yield of CH₄ with the sum of emissions and oxidation. Most of
524 the time, the emissions alone and/or the sum of emissions and oxidation were significantly
525 higher than the amount of CH₄ that was lost from the water column. At the Pääjärvi Lake in
526 Finland (López Bellido et al., 2009), the fact that measured or calculated emissions exceed the
527 loss of CH₄ in the water column was attributed to a probable underestimation of the CH₄
528 storage in the lake by under-sampling the shallow area of the lake. In this study, emissions,
529 storage and oxidation were estimated at the same stations, avoiding such sampling artefacts.
530 Therefore, it suggests that CH₄ is provided by lateral transport or by production in the flooded
531 soil and biomass (Guerin et al., 2008) at a higher rate than the total loss of CH₄ from the water
532 column by emissions and oxidation. This hypothesis could only be verified by a full CH₄
533 mass balance including production and total emissions from the reservoir, which is beyond
534 the scope of this article.

535 **4.3. Hot spot of emissions at the water intake (RES9)**

536 After the commissioning of the reservoir, the temperature and the oxygen and CH₄
537 concentrations were constant from the surface to the bottom of the reservoir at the vicinity of
538 the water intake. On the basis of physical modelling and measurements of water current
539 velocities (Chanudet et al., 2012), the vertical mixing at this station was attributed to the water
540 withdrawal at the intake generating turbulence and water currents over a surface area of 3
541 km². At this station, CH₄-rich water from the reservoir hypolimnion reached the surface and
542 led to diffusive fluxes up to 600 mmol m⁻² d⁻¹ in the WD-WW seasons (Figure 7b) whereas
543 fluxes are 3 orders of magnitude lower in the CD season. These high fluxes are the highest
544 reported at the surface of an aquatic ecosystem (Abril et al., 2005;Guerin et al.,
545 2006;Bastviken et al., 2011;Barros et al., 2011;Deshmukh et al., 2016). To the best of our
546 knowledge, this is the first time it is reported that the artificial mixing induced by the water
547 intakes upstream of a dam or a power station enhance significantly emissions. At NT2R, the
548 intake is located at the bottom of a narrow (130 m) and shallow channel (depth =9-20 m) on
549 the side of the reservoir (Figure S1). This design enhances horizontal water current velocities,

550 the vertical mixing and therefore the emissions. The existence of such a hotspot at other
551 reservoirs might be highly dependant on the design of the water intake (depth among other
552 parameters) and its effect on the hydrodynamics of the reservoir water column.

553 **4.4. Estimation of total diffusive fluxes from the reservoir**

554 Yearly emissions by diffusive fluxes peaked at more than 9 Gg(CH₄) in 2010 when the
555 reservoir was commissioned and they decreased down to \approx 5 Gg(CH₄) in 2011 and 2012
556 (Figure 9a and Table 3). Yearly integrated at the whole reservoir surface, these emissions
557 correspond to diffusive fluxes of 1.5 to 4 mmol m⁻² d⁻¹. These emissions are significantly
558 lower than diffusive fluxes measured at the Petit Saut Reservoir during the first two years
559 after flooding but similar to those determined in the following years (Abril et al., 2005) and
560 values reported for diffusive fluxes from tropical reservoirs in Barros et al. (2011). In absence
561 of the extreme emissions (both hotspots and hot moments), diffusive emissions from NT2R
562 would have been one order of magnitude lower than emissions from tropical reservoirs as
563 expected from the lower flooded biomass compare to Amazonian reservoirs (Descloux et al.,
564 2011). Due to the specific dynamic of diffusive fluxes at NT2R with hotspots and hot
565 moments, diffusion at the reservoir surface contribute 18 to 27% of total emissions (Table 3)
566 that is significantly higher than at other reservoirs tropical reservoirs where it was measured
567 (See also Deshmukh et al., 2016).

568 Most of the increase of CH₄ emissions by diffusive fluxes from 4 to 9 Gg(CH₄) between 2009
569 and 2010 is due to very significant emissions of 2-3 Gg(CH₄) at the water intake after the
570 commissioning of the reservoir and resulting artificial mixing (Figure 9a). This increase might
571 be overestimated because we have no measurements between Jan. and April but this
572 overestimation might be reasonable since those months are usually associated with the lowest
573 emissions of the year (Figure 9b). After the commissioning, the outgassing of CH₄ was
574 triggered by the artificial mixing generated by the withdrawal of water from the reservoir to
575 the turbines. Although the area under the influence of the water intake is less than 1% of the
576 total area of the reservoir, emissions at the water intake contributed between 13 and 25% of
577 total diffusive emissions and 4 to 10 % if considering both ebullition and diffusion,
578 disregarding the year 2009 (Table 3). It is worth to note that emissions at this site are only
579 significant within 3-5 month per year at the end of the WD season-beginning of the WW
580 season when the storage of CH₄ reach its maximum in the reservoir (Figure 9b). This new
581 hotspot equals 20 to 40% of downstream emissions and contributes between 3 and 7% of total

582 emissions from NT2R surface when including ebullition and downstream emissions (Table 3
583 and Deshmukh et al. (2016)). Localized perturbation of the hydrodynamics, especially in
584 lakes or reservoirs with CH₄-rich hypolimnion, can generate hotspots of emissions
585 contributing significantly to the total emissions from a given ecosystem. These hotspots could
586 be found upstream of dams and water intake in reservoirs but also around aeration stations
587 based on air injection or artificial mixing that could be used for improving water quality in
588 water bodies (Wüest et al., 1992).

589 The contribution of extreme diffusive fluxes (with daily values being > 5 up to 200 mmol m⁻²
590 d⁻¹) to total emission by diffusion range from 30 to 50% on a yearly basis (Figure 9a) and
591 from 40 up to 70% on a monthly basis (Figure 9b) although these hot moments represent less
592 than 10% of the observations during the monitoring. In the literature, the statistical
593 distribution of CH₄ emissions dataset always follows heavy-tailed and right skewed
594 distribution like the log-normal, the Generalized Pareto Distribution (Windsor et al.,
595 1992;Czepiel et al., 1993;Ramos et al., 2006;DelSontro et al., 2011) or loglogistic (this study)
596 which indicates that CH₄ emissions are always characterized by high episodic fluxes. The
597 quantification of emissions thus requires the highest spatial and temporal resolutions in order
598 to capture as many hot moments as possible. At a single station, there is a possibility that we
599 did not catch the peak of emissions but extreme emission events never lasted more than 2
600 months (3 consecutive sampling dates) and probably lasted less than 15 days most of the time
601 (Figure 8). The auto-correlation function of the concentration time series indicates that a
602 minimum sampling frequency of 1 month is required in this monomictic reservoirs for an
603 accurate description of the change in the surface concentrations and estimation of the
604 emissions (Figure S4). Although a better temporal resolution than 15 days or monthly would
605 probably improve the estimation of CH₄ emissions from this reservoir, a lower temporal
606 resolution could significantly affect (positively or negatively) the emission factor of this
607 reservoir that overturn gradually over several month. Therefore, the monthly frequency
608 defined for this specific reservoir is probably not applicable to every aquatic ecosystem,
609 especially in lakes or reservoirs that overturn within a week or less (Kankaala et al.,
610 2007;López Bellido et al., 2009;Schubert et al., 2012). However, it suggests that
611 quantification of emissions based on 2-4 campaigns in a year might significantly affect
612 emissions factors and carbon budgets of ecosystems under study.

613 **5. Conclusion**

614 The monitoring of CH₄ diffusive emissions every two weeks at nine stations revealed
615 complex temporal and spatial variations that could hardly been characterized by seasonal
616 sampling. The highest emissions occur sporadically during hot moments in the rainy season
617 and when the reservoir overturns. In the rainy season, they mostly occur in the inflow region
618 because the increase of the discharge of cool water from the reservoir tributaries contributes
619 to sporadic thermal destratification. During the reservoir overturn, extreme emissions occur
620 mostly in area far from inflows and outflows that are supposed to have the highest water
621 residence time. It shows that diffusive emissions can be sporadically as high as ebullition and
622 that these hot moments could contribute very significantly to the total emissions from natural
623 aquatic ecosystems and reservoirs. Our results suggest that sporadic emissions cannot be
624 integrated properly in the quantification of emissions and establishments of carbon budgets
625 based only on seasonal sampling (2-4 campaigns).

626 We also identified a new hotspot of emissions upstream of the water intake resulting from the
627 artificial destratification of the water column due to horizontal and vertical mixing generated
628 by the water withdrawal. In the case of the NT2R, emissions from this site contribute up to
629 25% of total diffusive emissions over less than 1% of the total reservoir area. We highly
630 recommend measurements of diffusive fluxes around water intakes (immediately upstream of
631 dams, typically) in order to evaluate if such results can be generalized.

632 **Acknowledgements**

633 The authors thank everyone who contributed to the NT2 monitoring programme, especially
634 the Nam Theun 2 Power Company (NTPC) and Electricité de France (EDF) for providing
635 financial, technical and logistic support. We are also grateful to the Aquatic Environment
636 Laboratory of the Nam Theun 2 Power Company whose Shareholders are EDF, Lao Holding
637 State Enterprise and Electricity Generating Public Company Limited of Thailand. CD
638 benefited from a PhD grant by EDF.

639

640 **References**

- 641 Abril, G., Guerin, F., Richard, S., Delmas, R., Galy-Lacaux, C., Gosse, P., Tremblay, A.,
642 Varfalvy, L., Dos Santos, M. A., and Matvienko, B.: Carbon dioxide and methane emissions
643 and the carbon budget of a 10-year old tropical reservoir (Petit Saut, French Guiana), *Global*
644 *Biogeochem. Cycles*, 19, 10.1029/2005gb002457, 2005.
- 645 Abril, G., Commarieu, M.-V., and Guerin, F.: Enhanced methane oxidation in an estuarine
646 turbidity maximum, *Limnol. Oceanogr.*, 52, 470-475, 2007.
- 647 Barros, N., Cole, J. J., Tranvik, L. J., Prairie, Y. T., Bastviken, D., Huszar, V. L. M., del
648 Giorgio, P., and Roland, F.: Carbon emission from hydroelectric reservoirs linked to reservoir
649 age and latitude, *Nature Geosci*, 4, 593-596, 2011.
- 650 Bastviken, D., Ejlertsson, J., and Tranvik, L.: Measurement of methane oxidation in lakes: A
651 comparison of methods, *Environ. Sci. Technol.*, 36, 3354-3361, 10.1021/es010311p, 2002.
- 652 Bastviken, D., Cole, J. J., Pace, M. L., and Van de Bogert, M. C.: Fates of methane from
653 different lake habitats: Connecting whole-lake budgets and CH₄ emissions, *J. Geophys. Res.-*
654 *Biogeosci.*, 113, G02024
655 10.1029/2007jg000608, 2008.
- 656 Bastviken, D., Tranvik, L. J., Downing, J. A., Crill, P. M., and Enrich-Prast, A.: Freshwater
657 Methane Emissions Offset the Continental Carbon Sink, *Science*, 331, 50,
658 10.1126/science.1196808, 2011.
- 659 Bedard, C., and Knowles, R.: Some properties of methane oxidation in a thermally stratified
660 lake, *Can. J. Fish. Aquat.Sci.*, 54, 1639-1645, 1997.
- 661 Borges, A. V., Delille, B., Schiettecatte, L. S., Gazeau, F., Abril, G., and Frankignoulle, M.:
662 Gas transfer velocities of CO₂ in three European estuaries (Randers Fjord, Scheldt, and
663 Thames), *Limnol. Oceanogr.*, 49, 1630-1641, 2004.
- 664 Chanudet, V., Descloux, S., Harby, A., Sundt, H., Hansen, B. H., Brakstad, O., Serca, D., and
665 Guerin, F.: Gross CO₂ and CH₄ emissions from the Nam Ngum and Nam Leuk sub-tropical
666 reservoirs in Lao PDR, *Sci. Total Environ.*, 409, 5382-5391, 10.1016/j.scitotenv.2011.09.018,
667 2011.
- 668 Chanudet, V., Fabre, V., and van der Kaaij, T.: Application of a three-dimensional
669 hydrodynamic model to the Nam Theun 2 Reservoir (Lao PDR), *J. Great Lakes Res.*, 38, 260-
670 269, <http://dx.doi.org/10.1016/j.jglr.2012.01.008>, 2012.
- 671 Chen, H., Wu, Y., Yuan, X., Gao, Y., Wu, N., and Zhu, D.: Methane emissions from newly
672 created marshes in the drawdown area of the Three Gorges Reservoir, *J. Geophys. Res.*, 114,
673 D18301, doi:10.1029/2009JD012410, 2009.
- 674 Chen, H., Yuan, X., Chen, Z., Wu, Y., Liu, X., Zhu, D., Wu, N., Zhu, Q. a., Peng, C., and Li,
675 W.: Methane emissions from the surface of the Three Gorges Reservoir, *J. Geophys. Res.*,
676 116, D21306, 10.1029/2011jd016244, 2011.
- 677 Czepiel, P. M., Crill, P. M., and Harriss, R. C.: Methane emissions from municipal
678 wastewater treatment processes, *Environ. Sci. Technol.*, 27, 2472-2477,
679 10.1021/es00048a025, 1993.
- 680 Delignette-Muller, M. L., Dutang, C., Pouillot, R., and Denis, J.-B.: An R Package for Fitting
681 Distributions, 1.0-4, 2015
- 682 DelSontro, T., McGinnis, D. F., Sobek, S., Ostrovsky, I., and Wehrli, B.: Extreme Methane
683 Emissions from a Swiss Hydropower Reservoir: Contribution from Bubbling Sediments,
684 *Environ. Sci. Technol.*, 44, 2419-2425, 10.1021/es9031369, 2010.
- 685 DelSontro, T., Kunz, M. J., Kempter, T., Wüest, A., Wehrli, B., and Senn, D. B.: Spatial
686 Heterogeneity of Methane Ebullition in a Large Tropical Reservoir, *Environ. Sci. Technol.*,
687 45, 9866-9873, 10.1021/es2005545, 2011.

688 Descloux, S., Chanudet, V., Poilvé, H., and Grégoire, A.: Co-assessment of biomass and soil
689 organic carbon stocks in a future reservoir area located in Southeast Asia, *Environ. Monit.*
690 *Assess.*, 173, 723-741, 10.1007/s10661-010-1418-3, 2011.

691 Descloux, S., Guedant, P., Phommachanh, D., and Luthi, R.: Main features of the Nam Theun
692 2 hydroelectric project (Lao PDR) and the associated environmental monitoring programmes,
693 *Hydroécol. Appl.*, 10.1051/hydro/2014005 2014, 2014.

694 Deshmukh, C., Serca, D., Delon, C., Tardif, R., Demarty, M., Jarnot, C., Meyerfeld, Y.,
695 Chanudet, V., Guedant, P., Rode, W., Descloux, S., and Guerin, F.: Physical controls on CH₄
696 emissions from a newly flooded subtropical freshwater hydroelectric reservoir: Nam Theun 2,
697 *Biogeosciences*, 11, 4251-4269, 10.5194/bg-11-4251-2014, 2014.

698 Deshmukh, C., Guérin, F., Labat, D., Pighini, S., Vongkhamsoo, A., Guédant, P., Rode, W.,
699 Godon, A., Chanudet, V., Descloux, S., and Serça, D.: Low methane (CH₄) emissions
700 downstream of a monomictic subtropical hydroelectric reservoir (Nam Theun 2, Lao PDR),
701 *Biogeosciences*, 13, 1919-1932, 10.5194/bg-13-1919-2016, 2016.

702 Dumestre, J. F., Guezennec, J., Galy-Lacaux, C., Delmas, R., Richard, S., and Labroue, L.:
703 Influence of Light Intensity on Methanotrophic Bacterial Activity in Petit Saut Reservoir,
704 French Guiana, *Appl. Environ. Microbiol.*, 65, 534-539, 1999.

705 Fernández, J. E., Peeters, F., and Hofmann, H.: Importance of the Autumn Overturn and
706 Anoxic Conditions in the Hypolimnion for the Annual Methane Emissions from a Temperate
707 Lake, *Environ. Sci. Technol.*, 48, 7297-7304, 10.1021/es4056164, 2014.

708 Galy-Lacaux, C., Delmas, R., Lambert, C., Dumestre, J. F., Labroue, L., Richard, S., and
709 Gosse, P.: Gaseous emissions and oxygen consumption in hydroelectric dams: A case study in
710 French Guyana, *Global Biogeochem. Cycles*, 11, 471-483, 1997.

711 Gross, J., and Ligges, U.: Tests for Normality (Nortest), 1.04-4, 2015

712 Guerin, F., Abril, G., Richard, S., Burban, B., Reynouard, C., Seyler, P., and Delmas, R.:
713 Methane and carbon dioxide emissions from tropical reservoirs: Significance of downstream
714 rivers, *Geophys. Res. Lett.*, 33, 10.1029/2006gl027929, 2006.

715 Guerin, F., and Abril, G.: Significance of pelagic aerobic methane oxidation in the methane
716 and carbon budget of a tropical reservoir, *J. Geophys. Res.-Biogeosci.*, 112,
717 10.1029/2006jg000393, 2007.

718 Guerin, F., Abril, G., Serca, D., Delon, C., Richard, S., Delmas, R., Tremblay, A., and
719 Varfalvy, L.: Gas transfer velocities of CO₂ and CH₄ in a tropical reservoir and its river
720 downstream, *J. Mar. Syst.*, 66, 161-172, 10.1016/j.jmarsys.2006.03.019, 2007.

721 Guerin, F., Abril, G., de Junet, A., and Bonnet, M.-P.: Anaerobic decomposition of tropical
722 soils and plant material: Implication for the CO₂ and CH₄ budget of the Petit Saut Reservoir,
723 *Appl. Geochem.*, 23, 2272-2283, 10.1016/j.apgeochem.2008.04.001, 2008.

724 Jahne, B., Munnich, K. O., Bosinger, R., Dutzi, A., Huber, W., and Libner, P.: On the
725 parameters influencing air-water gas-exchange, *J. Geophys. Res. Oceans*, 92, 1937-1949,
726 1987.

727 Kankaala, P., Taipale, S., Nykanen, H., and Jones, R. I.: Oxidation, efflux, and isotopic
728 fractionation of methane during autumnal turnover in a polyhumic, boreal lake, *J. Geophys.*
729 *Res.-Biogeosci.*, 112, G02003
730 10.1029/2006jg000336, 2007.

731 Kemenes, A., Forsberg, B. R., and Melack, J. M.: Methane release below a tropical
732 hydroelectric dam, *Geophys. Res. Lett.*, 34, L12809 10.1029/2007gl029479, 2007.

733 López Bellido, J., Tulonen, T., Kankaala, P., and Ojala, A.: CO₂ and CH₄ fluxes during
734 spring and autumn mixing periods in a boreal lake (Pääjärvi, southern Finland), *J. Geophys.*
735 *Res.-Biogeosci.*, 114, G04007, 10.1029/2009JG000923, 2009.

736 MacIntyre, S., Jonsson, A., Jansson, M., Aberg, J., Turney, D. E., and Miller, S. D.: Buoyancy
737 flux, turbulence, and the gas transfer coefficient in a stratified lake, *Geophys. Res. Lett.*, 37,
738 L24604, 10.1029/2010GL044164, 2010.

739 Maeck, A., DelSontro, T., McGinnis, D. F., Fischer, H., Flury, S., Schmidt, M., Fietzek, P.,
740 and Lorke, A.: Sediment Trapping by Dams Creates Methane Emission Hot Spots, *Environ.*
741 *Sci. Technol.*, 47, 8130-8137, 10.1021/es4003907, 2013.

742 McClain, M. E., Boyer, E. W., Dent, C. L., Gergel, S. E., Grimm, N. B., Groffman, P. M.,
743 Hart, S. C., Harvey, J. W., Johnston, C. A., Mayorga, E., McDowell, W. H., and Pinay, G.:
744 Biogeochemical hot spots and hot moments at the interface of terrestrial and aquatic
745 ecosystems, *Ecosystems*, 6, 301-312, 10.1007/s10021-003-0161-9, 2003.

746 Musenze, R. S., Grinham, A., Werner, U., Gale, D., Sturm, K., Udy, J., and Yuan, Z.:
747 Assessing the Spatial and Temporal Variability of Diffusive Methane and Nitrous Oxide
748 Emissions from Subtropical Freshwater Reservoirs, *Environ. Sci. Technol.*, 48, 14499-14507,
749 10.1021/es505324h, 2014.

750 NTPC: Environmental Assessment and Management Plan - Nam Theun 2 Hydroelectric
751 Project. Nam Theun 2 Power Company, NTPC (Nam Theun 2 Power Company), Vientiane,
752 212, 2005.

753 Pacheco, F. S., Soares, M. C. S., Assireu, A. T., Curtarelli, M. P., Roland, F., Abril, G., Stech,
754 J. L., Alvalá, P. C., and Ometto, J. P.: The effects of river inflow and retention time on the
755 spatial heterogeneity of chlorophyll and water-air CO₂ fluxes in a tropical hydropower
756 reservoir, *Biogeosciences*, 12, 147-162, 10.5194/bg-12-147-2015, 2015.

757 R Development Core Team: R: A Language and Environment for Statistical Computing, R
758 Foundation for Statistical Computing, Vienna, Austria, 3-900051-07-0, 2008

759 Ramos, F. M., Lima, I. B. T., Rosa, R. R., Mazzi, E. A., Carvalho, J. o. C., Rasera, M. F. F.
760 L., Ometto, J. P. H. B., Assireu, A. T., and Stech, J. L.: Extreme event dynamics in methane
761 ebullition fluxes from tropical reservoirs, *Geophys. Res. Lett.*, 33, L21404,
762 10.1029/2006gl027943, 2006.

763 Schubert, C., Lucas, F., Durisch-Kaiser, E., Stierli, R., Diem, T., Scheidegger, O., Vazquez,
764 F., and Müller, B.: Oxidation and emission of methane in a monomictic lake (Rotsee,
765 Switzerland), *Aquat. Sci.*, 72, 455-466, 10.1007/s00027-010-0148-5, 2010.

766 Schubert, C. J., Diem, T., and Eugster, W.: Methane Emissions from a Small Wind Shielded
767 Lake Determined by Eddy Covariance, Flux Chambers, Anchored Funnels, and Boundary
768 Model Calculations: A Comparison, *Environ. Sci. Technol.*, 46, 4515-4522,
769 10.1021/es203465x, 2012.

770 Sobek, S., DelSontro, T., Wongfun, N., and Wehrli, B.: Extreme organic carbon burial fuels
771 intense methane bubbling in a temperate reservoir, *Geophys. Res. Lett.*, 39, L01401,
772 10.1029/2011gl050144, 2012.

773 St Louis, V. L., Kelly, C. A., Duchemin, E., Rudd, J. W. M., and Rosenberg, D. M.: Reservoir
774 surfaces as sources of greenhouse gases to the atmosphere: A global estimate, *Bioscience*, 50,
775 766-775, 2000.

776 Sturm, K., Yuan, Z., Gibbes, B., Werner, U., and Grinham, A.: Methane and nitrous oxide
777 sources and emissions in a subtropical freshwater reservoir, South East Queensland, Australia,
778 *Biogeosciences*, 11, 5245-5258, 10.5194/bg-11-5245-2014, 2014.

779 Teodoru, C. R., Bastien, J., Bonneville, M.-C., del Giorgio, P. A., Demarty, M., Garneau, M.,
780 Hélie, J.-F., Pelletier, L., Prairie, Y. T., Roulet, N. T., Strachan, I. B., and Tremblay, A.: The
781 net carbon footprint of a newly created boreal hydroelectric reservoir, *Global Biogeochem.*
782 *Cycles*, 26, GB2016, 10.1029/2011gb004187, 2012.

783 Utsumi, M., Nojiri, Y., Nakamura, T., Nozawa, T., Otsuki, A., and Seki, H.: Oxidation of
784 dissolved methane in a eutrophic, shallow lake: Lake Kasumigaura, Japan, *Limnol.*
785 *Oceanogr.*, 43, 471-480, 1998a.

786 Utsumi, M., Nojiri, Y., Nakamura, T., Nozawa, T., Otsuki, A., Takamura, N., Watanabe, M.,
787 and Seki, H.: Dynamics of dissolved methane and methane oxidation in dimictic Lake Nojiri
788 during winter, *Limnol. Oceanogr.*, 43, 10-17, 1998b.
789 Wanninkhof, R.: Relationship between wind-speed and gas-exchange over the ocean, *J.*
790 *Geophys. Res. Oceans*, 97, 7373-7382, 1992.
791 Windsor, J., Moore, T. R., and Roulet, N. T.: Episodic fluxes of methane from subarctic fens,
792 *Can. J. Soil Sci.*, 72, 441-452, doi:10.4141/cjss92-037, 1992.
793 Wüest, A., Brooks, N. H., and Imboden, D. M.: Bubble plume modeling for lake restoration,
794 *Water Resour. Res.*, 28, 3235-3250, 10.1029/92WR01681, 1992.
795 Yamamoto, S., Alcauskas, J. B., and Crozier, T. E.: Solubility of methane in distilled water
796 and seawater, *J. Chem. Eng. Data*, 21, 78-80, 10.1021/je60068a029, 1976.
797 Zheng, H., Zhao, X. J., Zhao, T. Q., Chen, F. L., Xu, W. H., Duan, X. N., Wang, X. K., and
798 Ouyang, Z. Y.: Spatial-temporal variations of methane emissions from the Ertan hydroelectric
799 reservoir in southwest China, *Hydrol. Processes*, 25, 1391-1396, 10.1002/hyp.7903, 2011.
800
801

802
803
804

Table 1: Characteristics of the nine monitoring stations in the Nam Theun 2 Reservoir

Station	Depth (min-max) (m)	Flooded ecosystem ¹	Hydrology	Water residence time index ²
RES1	25.4-35	Dense forest	100 m upstream of the Nakai Dam	**
RES2	18.4-28	Dense forest	Thalweg of the Nam Theun River	**
RES3	6.4-16	Dense forest	Embayment	***
RES4	17.4-27	Degraded forest	Confluence Nam Theun-Nam Xot Rivers	**
RES5	8.4-18	Degraded forest	Aside from the main stream	**
RES6	15.4-25	Degraded forest	Thalweg of the Nam Theun River	*
RES7	5.4-15	Swamp	Between inflows and water intake	*
RES8	11.4-21	Agricultural soils	Between inflows and water intake	*
RES9	9.4-19	Civil construction	Water intake	*

805 ¹Descloux et al. (2011)

806 ²Water renewal index in arbitrary units, (***) stands for longer residence time, (**) for
807 average residence times and (*) for shorter residence times than average for the whole
808 reservoir

809

810

811 Table 2 : Median, average, ranges and proportion of diffusive fluxes (F_{CH_4}) < 1 and > 5 mmol
812 $m^{-1} d^{-1}$ for three seasons

813

Station		Warm Dry (WD)	Warm Wet (WW)	Cool Dry (CD)
RES1-RES8	n	212	252	217
	range	0.01-102.59	0.01-201.86	0.01-94.64
	median	1.08	0.64	0.20
	Average \pm SD	2.23 \pm 7.37	3.12 \pm 14.58	3.04 \pm 12.89
	% $F_{CH_4} < 1$	48%	63%	86%
	% $F_{CH_4} > 5$	6.6%	7.5%	7.4%
	Mediane $F > 5$	10.67	13.80	23.75
	Average $F > 5$	16.69 \pm 25.04	30.23 \pm 45.99	36.45 \pm 33.19
RES9	n	39	45	36
	range	0.24-342.00	0.03-605.38	0.07-17.62
	median	40.81	1.23	0.48
	average \pm SD	83.33 \pm 15.57	78.58 \pm 24.73	2.21 \pm 0.69

814

815

816 Table 3: Methane emissions from the Nam Theun 2 Reservoir between 2009 and 2012.

Gg(CH ₄) year ⁻¹	2009	2010	2011	2012
Emission from reservoir				
Diffusion at RES9 only	0.02±0.01	2.33±0.21	0.86±0.12	0.66±0.11
Total diffusion	4.45±1.01	9.34±2.32	3.71±0.81	4.95±1.09
Contribution of RES9 to diffusion (%)	0.4	24.9	23.2	13.3
Ebullition ¹	11.21±0.16	14.39±0.11	14.68±0.10	12.29±0.09
Total emissions from reservoir (Ebullition + diffusion at all stations)	15.66±1.02	23.73±2.32	18.39±0.82	17.25±1.09
Contribution of RES9 (%) to total emissions from reservoir	0.1	9.8	4.7	3.8
Total downstream emissions²	7.79±0.90	10.73±0.83	2.29±0.41	2.00±0.32
Total emissions (reservoir + downstream)	23.45±1.36	34.46±2.46	20.67±0.92	19.24±1.14
Contribution of diffusion to total emission	19%	27%	18%	26%
Contribution of RES9 to total (%)	<0.1	6.8	4.2	3.4

817 ¹Deshmukh et al. (2014)818 ²Deshmukh et al. (2016)

819

820

821
822 Figure captions

823

824 Figure 1: Map of the sampling stations and civil structures at the Nam Theun 2 Reservoir
825 (Lao PDR).

826

827 Figure 2: Variations of (a) surface of the reservoir (km^2), volume of water (km^3) and water
828 level (masl) at the Nam Theun 2 Reservoir between January 2009 and December 2012.

829

830 Figure 3: Vertical profiles of temperature ($^{\circ}\text{C}$), oxygen ($\mu\text{mol L}^{-1}$) and methane ($\mu\text{mol L}^{-1}$) at
831 the stations RES1, RES3, RES7, RES8 and RES9 in the Nam Theun 2 Reservoir.

832 Representative profile of the years 2010 (circle), 2011 (square) and 2012 (triangle) are given
833 for each seasons: cool dry in blue, warm dry in red, and warm wet in grey. Note that for the
834 stations RES3 and RES9, the scale is different for the vertical profiles of CH_4 .

835

836 Figure 4: (a) Stratification index (ΔT , see text), (b) O_2 concentration in the hypolimnion
837 ($\mu\text{mol L}^{-1}$), (c) CH_4 concentration in the hypolimnion ($\mu\text{mol L}^{-1}$) and (d) CH_4 storage in the
838 water column ($\text{Gg}(\text{CH}_4) \text{ month}^{-1}$, bars) and water residence time (days, black line with circles)
839 in the Nam Theun 2 Reservoir (Lao PDR) between 2009 and 2012. The red, grey and blue
840 colours indicate the warm dry (WD), warm wet (WW) and cool dry (CD) seasons,
841 respectively. For the panels (a), (b) and (c), the boxes show the median and the interquartile
842 range, the whiskers denote the full range of values and the plus sign (+) denotes the mean.

843

844 Figure 5: Seasonal variations between 2010 and 2012 of the depth-integrated aerobic CH_4
845 oxidation ($\text{mmol m}^{-2} \text{ d}^{-1}$) at the stations RES1-RES8 calculated from the aerobic oxidation
846 rates determined by (Deshmukh et al., 2016). WD stands for warm dry (in red), WW for
847 warm wet (in grey) and CD for cool dry (in blue). The boxes show the median and the
848 interquartile range, the whiskers denote the full range of values and the plus sign (+) denotes
849 the mean.

850

851 Figure 6: Frequency distribution of the log of CH_4 concentrations ($\mu\text{mol L}^{-1}$) at the nine
852 monitoring stations of the Nam Theun 2 Reservoir. The red, grey and blue colours indicate the
853 warm dry (WD), warm wet (WW) and cool dry (CD) seasons, respectively.

854

855 Figure 7: (a) Surface concentrations and (b) diffusive fluxes between June 2009 and
856 December 2012 at the station RES9 located at the water intake. Julian day 0 is 1st of January,
857 2009. The red, grey and blue colours indicate the warm dry (WD), warm wet (WW) and cool
858 dry (CD) seasons, respectively.

859

860 Figure 8: (a, d, g, j) stratification index (ΔT , red line, see text) and diffusive fluxes, (b,e,h,k)
861 CH_4 storage and (c,f,i,l) depth-integrated aerobic CH_4 oxidation ($\text{mmol m}^{-2} \text{d}^{-1}$, black line)
862 calculated from the aerobic oxidation rates determined by (Deshmukh et al., 2016) and ΔT
863 (red line) between June 2009 and December 2012 at the stations RES1, RES3, RES7 and
864 RES8 at the Nam Theun 2 Reservoir. Julian day 0 is 1st of January, 2009. The red, grey and
865 blue colour dots indicate the warm dry (WD), warm wet (WW) and cold dry (CD) seasons,
866 respectively.

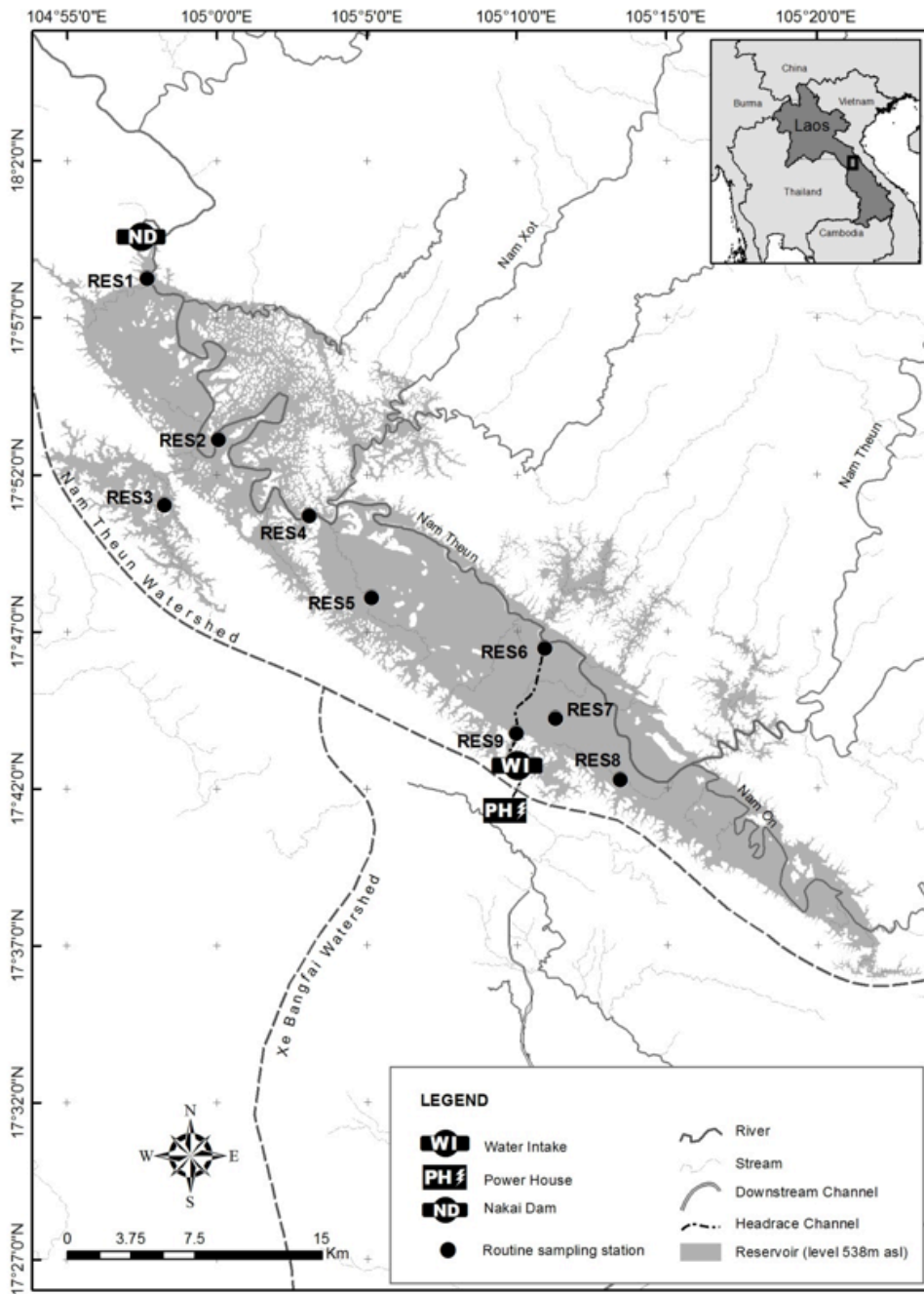
867

868 Figure 9: (a) Total emissions by diffusive fluxes in 2009, 2010, 2011 and 2012, and (b)
869 monthly emissions by diffusive fluxes between May 2009 and December 2012. Emissions
870 from RES9 (water intake) are shown in black, emissions resulting from diffusive fluxes lower
871 than $5 \text{ mmol m}^{-2} \text{d}^{-1}$ from the stations RES1 to RES8 are shown in white and emissions
872 resulting from diffusive fluxes higher than $5 \text{ mmol m}^{-2} \text{d}^{-1}$ from the stations RES1-RES8 are
873 shown in grey.

874

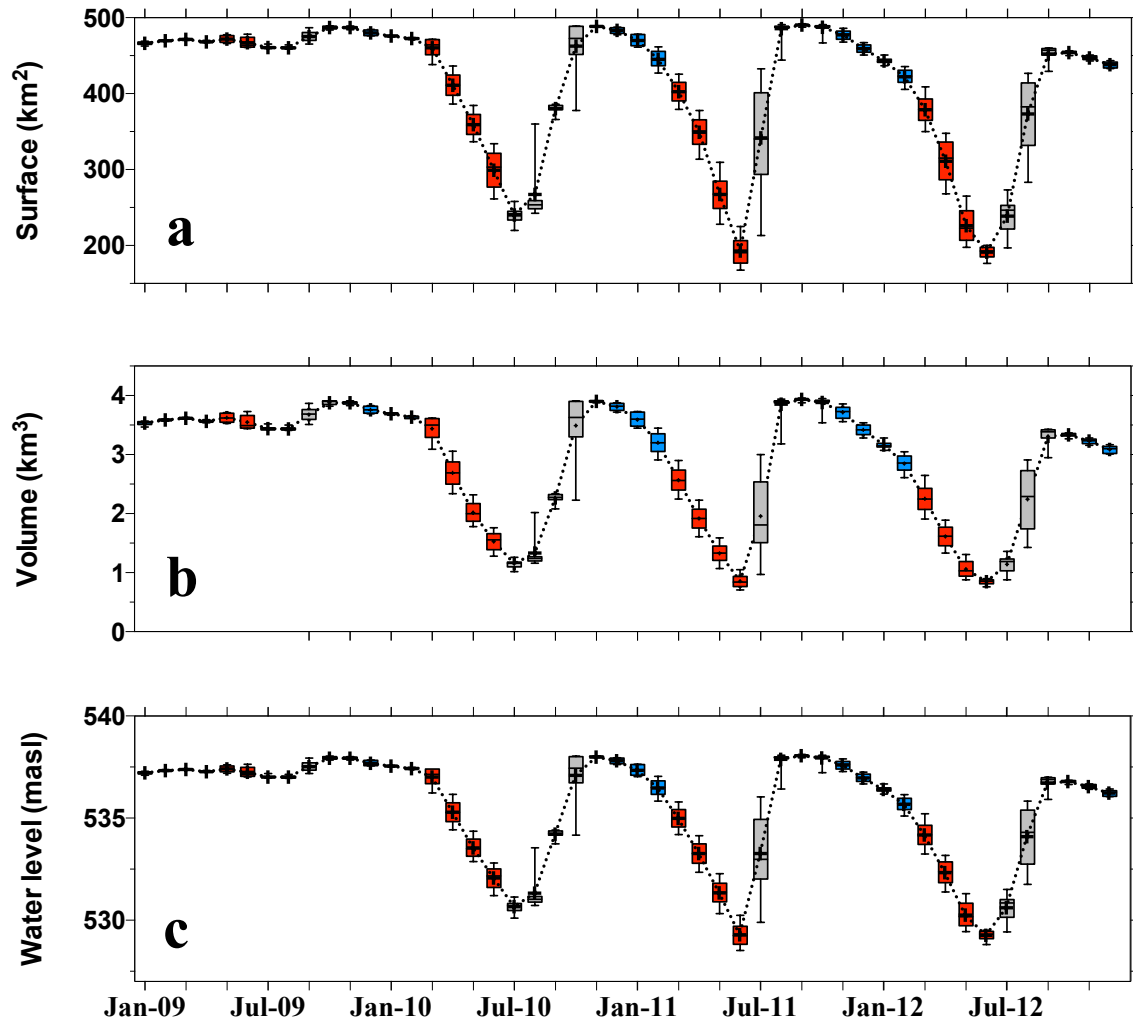
875

876
877 Figure 1
878



879
880
881

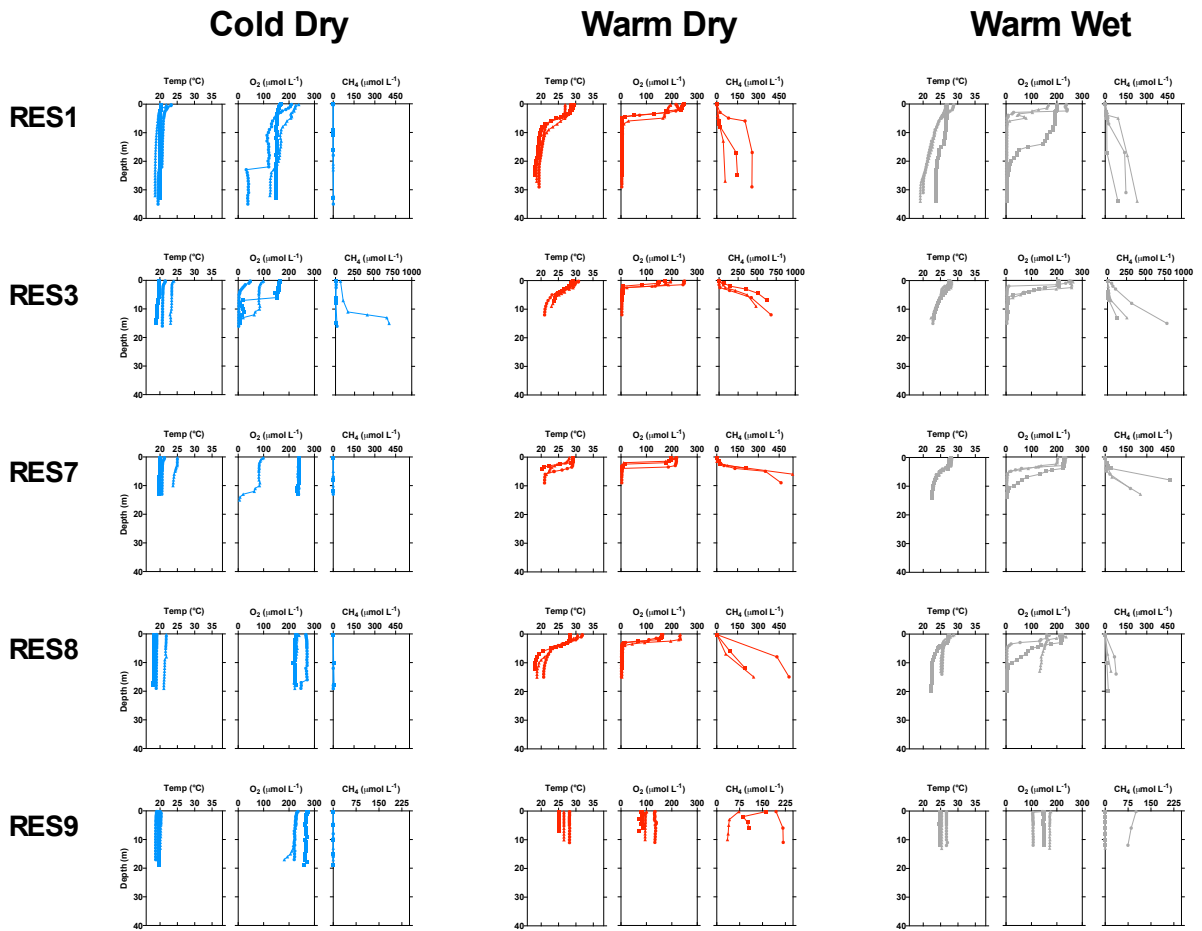
882 Figure 2
883



884
885

886 Figure 3

887

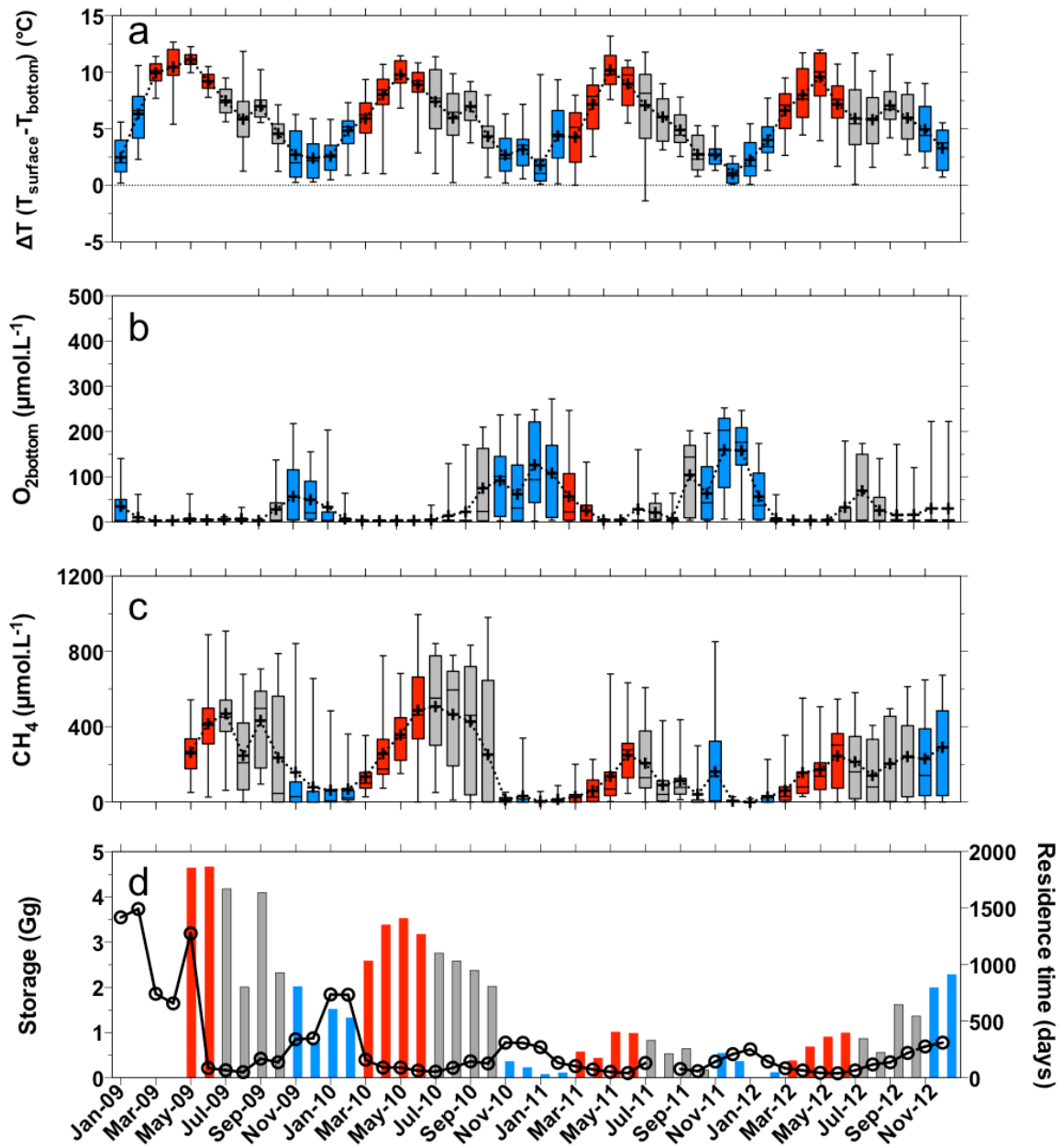


888

889

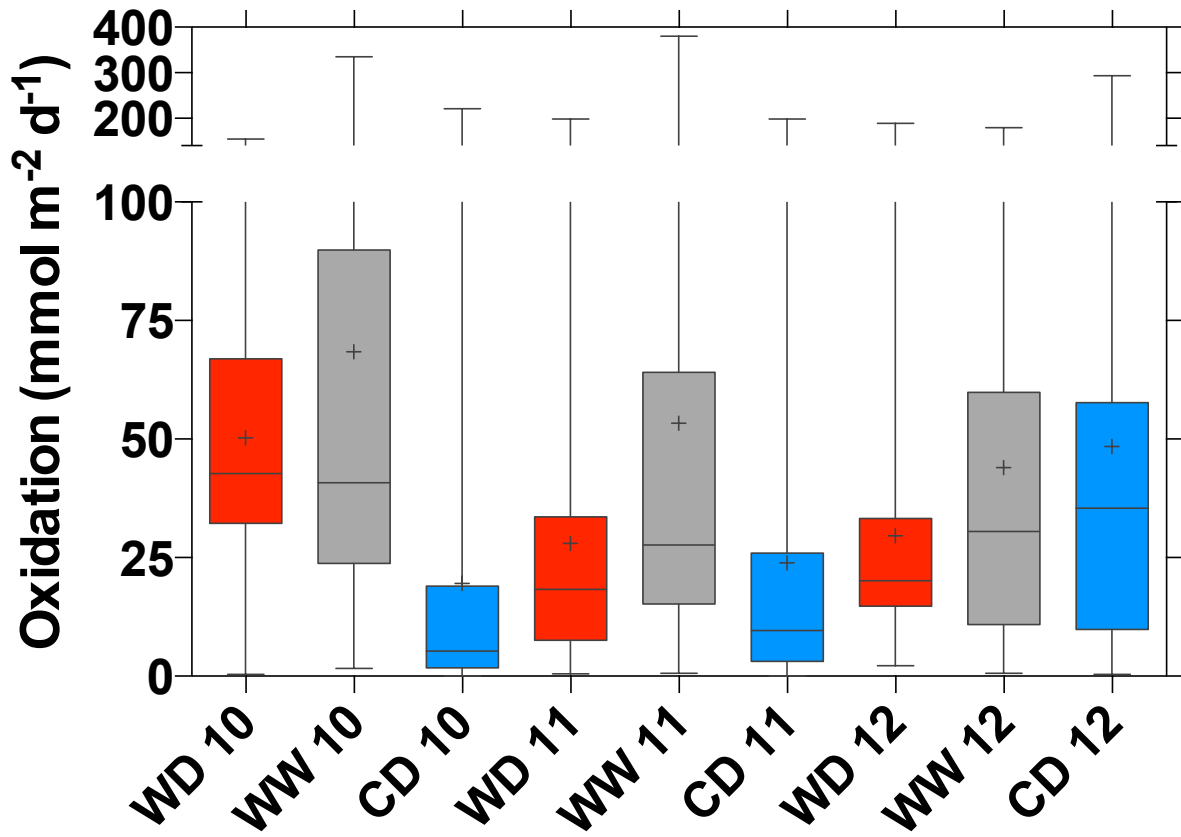
890

891
 892 Figure 4
 893



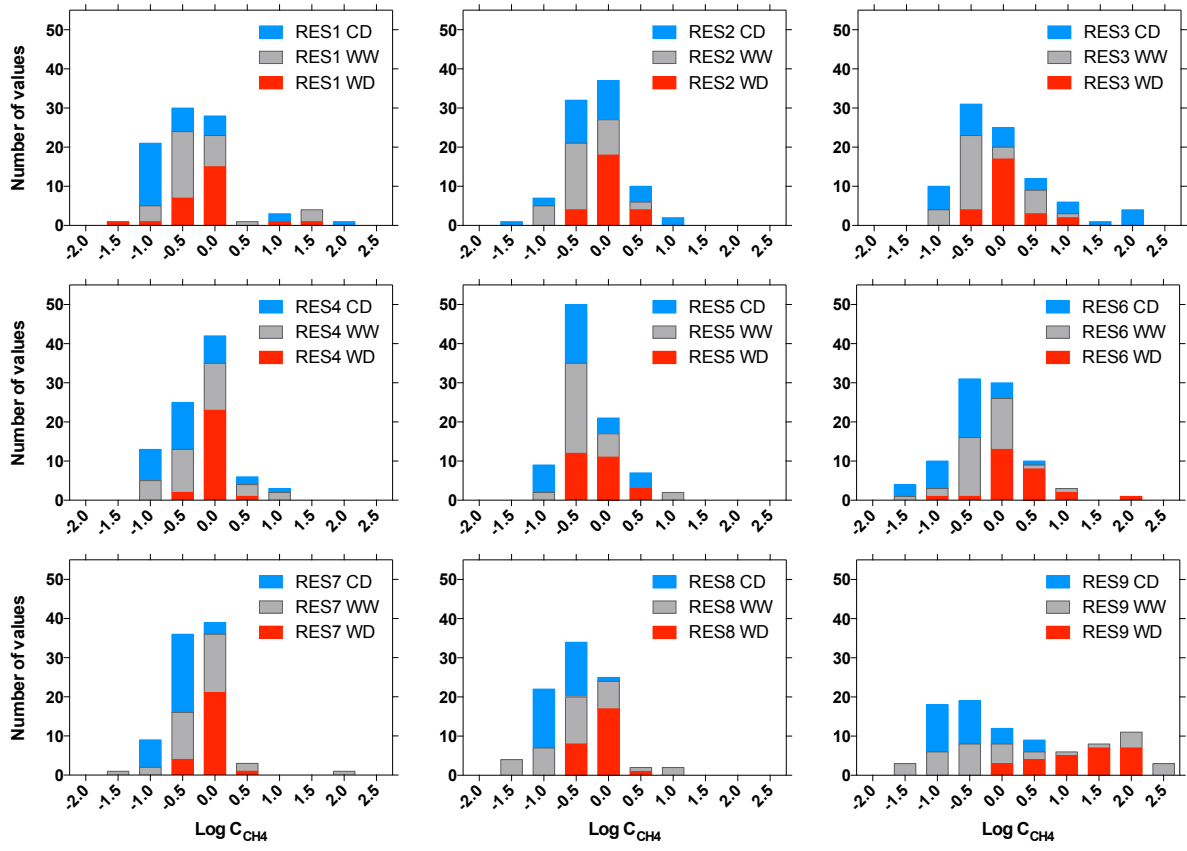
894
 895
 896

897
898 Figure 5
899



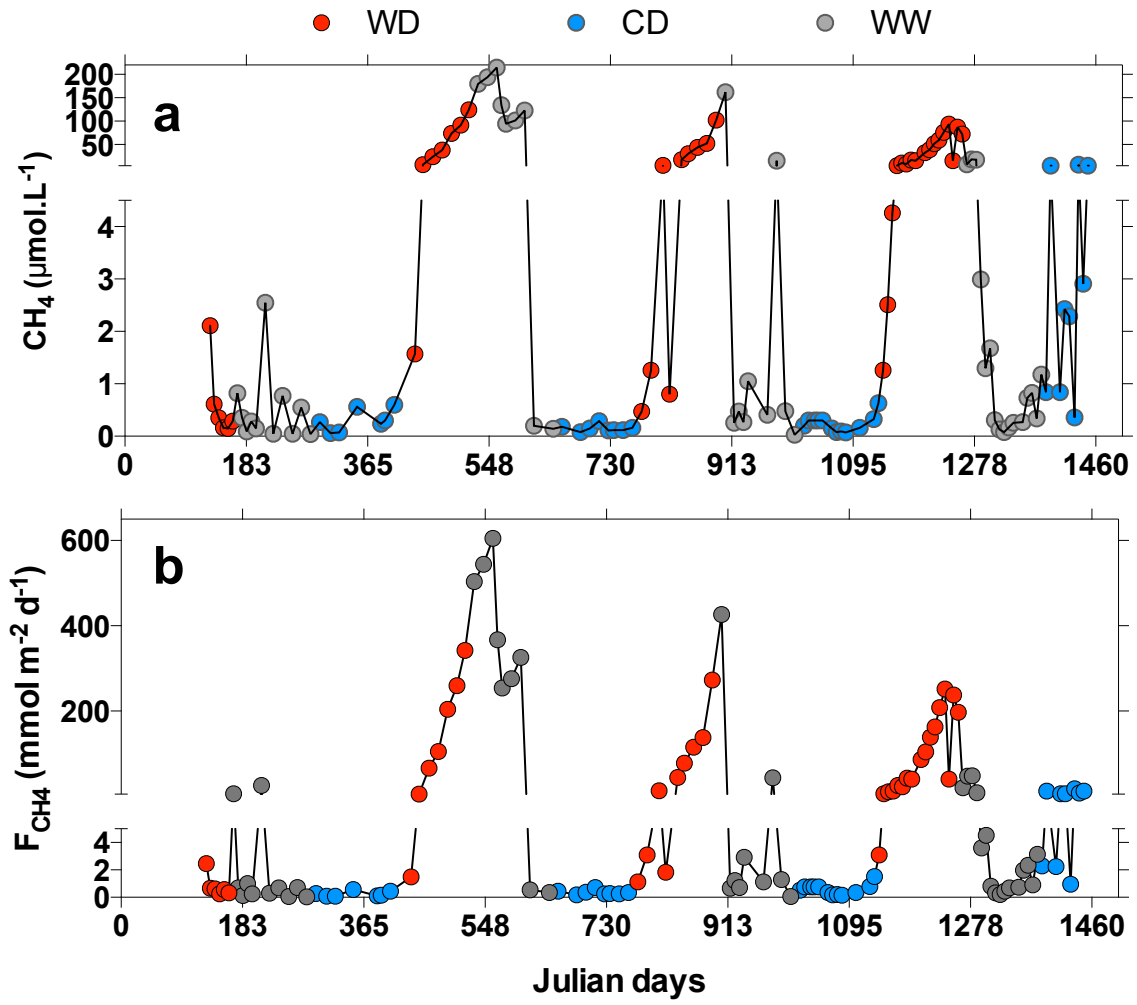
900
901
902

903
904 Figure 6
905



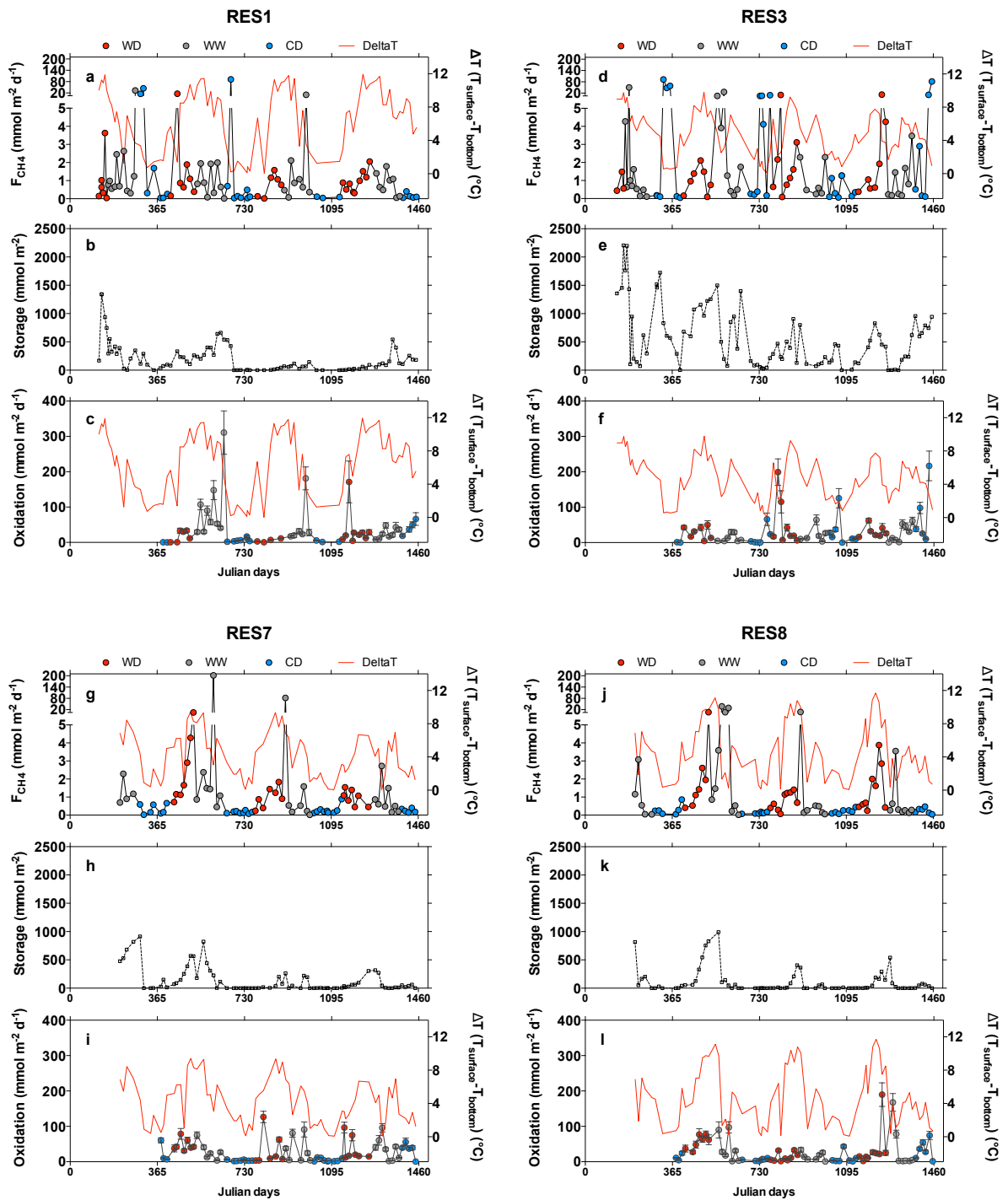
906
907
908

909
910 Figure 7
911



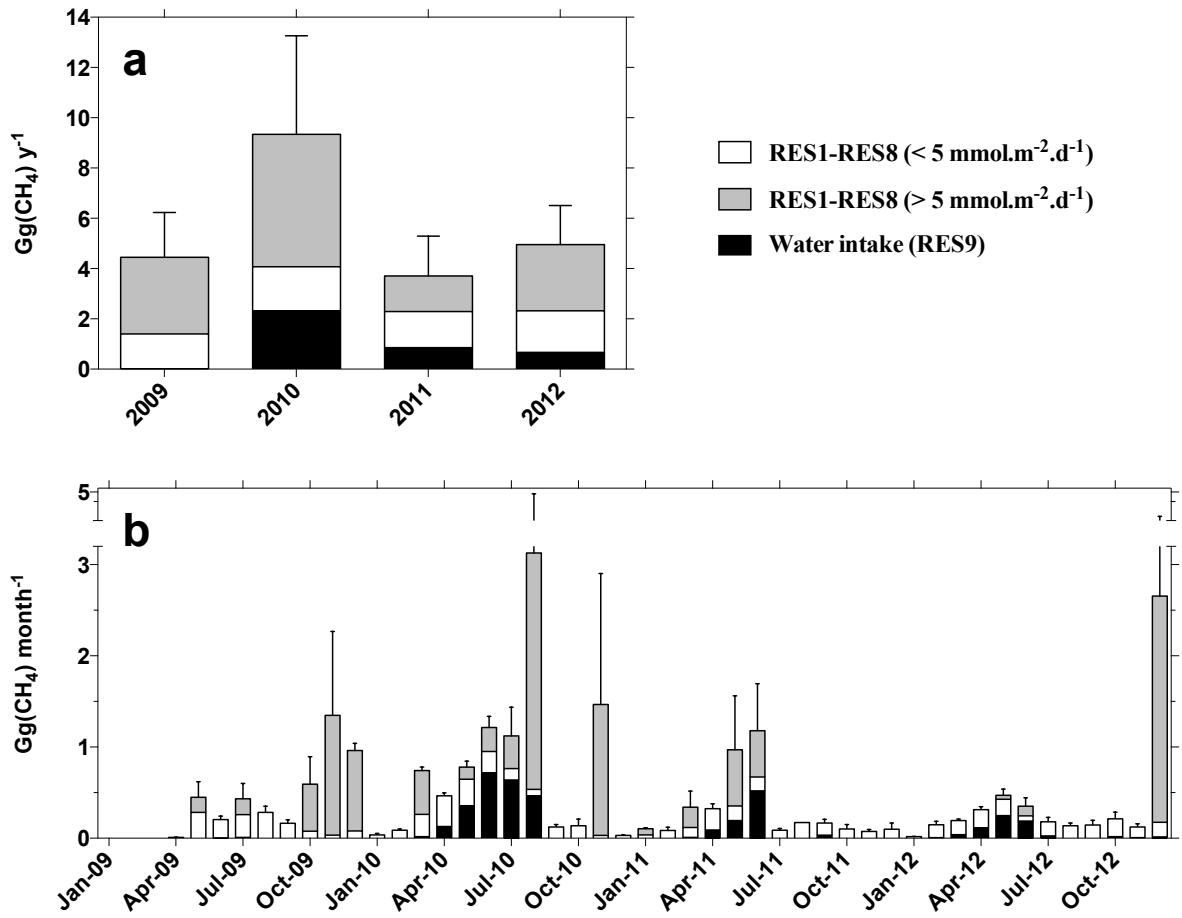
912
913
914

915
916 Figure 8
917



918
919
920

921
922 Figure 9
923



924